R. & M. No. 3522

MINISTRY OF TECHNOLOGY

AERONAUTICAL RESEARCH COUNCIL

REPORTS AND MEMORANDA

Real-Air Effects in Propelling Nozzles

By J. C. Ascough

LONDON: HER MAJESTY'S STATIONERY OFFICE
1968

PRICE 18*s.* 0*d.* NET

Real-Air Effects in Propelling Nozzles

By J. C. Ascough

Reports and Memoranda No. 3522*
September, 1966

Summary.

Properties of 'Real Air' in isentropic nozzle flow are compared with those of either 'Classic Air' for which $\gamma = 1{\cdot}4$ exactly or 'Ideal Air' for which γ may vary, but which obeys the Ideal Gas law $Pv = RT$.

Having shown that there is little difference between Classic Air and Ideal Air in the total temperature range from 270 to 400 deg K, the present results are presented as ratios of Real Air/Classic Air mass-flow intensity, and again as ratios of Real Air/Classic Air isentropic velocity. Operating conditions cover pressure ratios from 2 to 100, levels of inlet total pressure of 1, 4, 7 and 10 atm, and levels of inlet total temperature of 270, 290, 300, 350 and 400 deg K.

At inlet conditions of 10 atm and 290 deg K, Real Air isentropic velocity falls about 0·4 per cent below Classic Air, while Real Air mass-flow intensity rises about 0·6 per cent above Classic Air.

Strictly, the calculated results are for expansion of the respective fluids over exactly the same pressure ratio, which requires a flexible nozzle, but fixed nozzle operation is discussed.

LIST OF CONTENTS

*Replaces N.G.T.E. R.285—A.R.C. 28 513.

LIST OF CONTENTS—*continued*

LIST OF APPENDICES

LIST OF ILLUSTRATIONS

1. *Introduction.*

A convenient standard by which the efficiency of a propelling nozzle may be judged is the thrust produced by isentropic expansion of a reference gas. The usual reference fluids, either Ideal Air* or Classic Air*, are not suitable for accurate comparisons when the nozzle inlet pressure is high and the inlet temperature is low, as for many model test experiments. Under these conditions a more appropriate reference fluid is Real Air*.

A previous Note[1] examined the magnitude of the Real Air effect in model propelling nozzles using the data in Hilsenrath's tables[2] for Real Gas properties. In these earlier calculations, by means of desk machine, it was found necessary to avoid pressure-wise interpolations in the tables and so only a skeleton array of results was possible at that time.

More recently, calculations have been made by R. C. Johnson[3] on the effect of Real Gas upon the isentropic mass-flow intensity within a convergent nozzle, for a number of different gases, including air. His preliminary calculations also made use of Hilsenrath's tables to fit temperature polynomials which were used to calculate both the virial coefficients for the equation of state and to calculate the Ideal Gas specific heats. Thence his main computer program proceeded without further reference to the tables, being based upon Real Gas theory. Ratios of Real Gas to Ideal Gas mass-flow intensity were plotted for nozzle pressure ratios up to 2 – i.e., just greater than the critical or choking ($M = 1$) pressure ratio.

The opportunity has now been taken, as described in the present Report, to extend the calculations of Reference 1 with the aid of an electronic computer. Tedious pressure-wise interpolations were now possible although, in the event, these interpolations turned out to be numerically unstable and it became necessary to fall back on Real Air theory for this part of the calculations.

Ratios of Real Air to Classic Air isentropic mass flow intensity were to be checked against Johnson's results at the low pressure ratios (up to 2). Then for the wider range of interest for propelling nozzles (i.e., pressure ratios up to 100) results would be obtained on Real Air to Classic Air isentropic thrust ratio.

2. *Definitions.*

Types of air are classified according to the definitions of Reference 1 which are repeated here for convenience. For inlet temperatures around 300 deg K there is little difference between Classic Air and Ideal Air – in fact Johnson has used the word 'ideal' where the present text would have preferred 'classic'.

2.1. *Classic Air.*

A mixture of diatomic gases in which the internal energy consists of the translational and rotational modes only, the energy levels being fully established. The specific heats are constant at the values:

$$C_p = 3{\cdot}5\,R \tag{1}$$

and

$$C_v = 2{\cdot}5\,R \tag{2}$$

and so the ratio of the specific heats is constant at the value:

$$\gamma = \frac{C_p}{C_v} = 1{\cdot}4. \tag{3}$$

2.2. *Ideal Air.*

A mixture of gases that obeys the Ideal Gas law:

$$Pv = R\,T \tag{4}$$

---

*For definitions of Classic Air, Ideal Air, Real Air *see* Sections 2.1, 2.2, 2.3.

The Ideal Air specific heat C_p^0 varies with temperature, but is independent of pressure (it is equal to the Real Gas C_p at low pressure). Ideal Gas C_v^0 is given by:

$$C_p^0 - C_v^0 = R \tag{5}$$

where R is a constant for the gas.

Since C_p^0 (and C_v^0) varies with temperature, the specific heat ratio:

$$\gamma^0 = \frac{C_p^0}{C_v^0} = \frac{C_p^0}{C_p^0 - R} \tag{6}$$

also varies with temperature, but not with pressure.

2.3. *Real Air.*

A mixture of gases that obeys the Real Gas law:

$$Pv = ZR\,T. \tag{7}$$

Here, Z is the Real Gas compressibility factor which suffers the greatest departure from unity at low temperature and high pressure.

Real Air specific heat C_p varies with both temperature and pressure. The difference of specific heats is not equal to R, but is given by:

$$C_p - C_v = T\left(\frac{\partial P}{\partial T}\right)_v \left(\frac{\partial v}{\partial T}\right)_P \tag{8}$$

together with Equation (7).

The ratio of the specific heats varies both with temperatures and pressure.

3. *System of Units and Notation.*

The equations in this Report have been written within the framework of the m.k.s. system, the units of which are listed in the List of Symbols.

Of the innumerable variations in use within the ft.lb.s. system, the one quoted in the List of Symbols – the fundamental mechanical ft.lb.s. system – is self-consistent and can be compared with m.k.s.

Entropy and enthalpy data are tabulated by Hilsenrath in non-dimensional form as S/R and $(H - E_0^0)/R\,T_0$ respectively. However, to avoid excessive complication in Appendices III and IV the Notation S and H is used there to denote these non-dimensional quantities.

4. *Calculation Methods.*

4.1. *Basic Principles for Propelling-nozzle Thrust.*

Referring to Figure 1 the gross (gauge) thrust of a propelling nozzle is given by:

$$X_G = Q\,V^e + A^e\,(P_s^e - P_\infty) \tag{9}$$

where the index $^{(e)}$ denotes 'in the exit plane'.

Dividing by $Q\sqrt{T_t}$ we obtain the specific (gauge) gross thrust:

$$\frac{X_G}{Q\sqrt{T_t}} = \frac{V^e}{\sqrt{T_t}} + \frac{A^e}{Q\sqrt{T_t}}(P_s^e - P_\infty). \tag{10}$$

When operating a 'fixed nozzle' at the design pressure ratio (D.P.R.), the static pressure in the nozzle exit plane, P_s^e, is equal to ambient pressure P_∞ so that we obtain the specific thrust at D.P.R. from Equation (10):

$$\left[\frac{X_G}{Q\sqrt{T_t}}\right]_{\text{DPR}} = \frac{V^e}{\sqrt{T_t}}. \tag{11}$$

With a 'flexible nozzle', the area ratio can in principle be adjusted so that any pressure ratio becomes the D.P.R. The essential thing is that

$$r_{\text{DPR}} = \left[\frac{P_t}{P_s^e}\right]_{\text{DPR}} = \frac{P_t}{P_\infty} \tag{12}$$

i.e.

$$P_{s,\text{DPR}}^e = P_\infty \tag{13}$$

The isentropic relationship between velocity and enthalpy is shown in Appendix I to be:

$$V = \sqrt{2(H_t - H_s)}. \tag{14}$$

Equation (14) can be used for either Real Air or Ideal Air. The enthalpy difference for Real Air is discussed in Section 4.2. and Appendix III, while for Ideal Air it is discussed in Section 4.3. and Appendix IV.

4.2. *Real Air Isentropic Velocity and Mass-flow Intensity.*

Details of the calculation are given in Appendix III for the computational path ABCD illustrated in Figure 2.

Briefly, the method is to 'interpolate' the tables of Hilsenrath to find the temperature $T_{s,\text{REAL}}$ at the pressure P_s for the given pressure ratio, at which the entropy S_s is equal to the initial entropy S_t. Having found $T_{s,\text{REAL}}$, the tables are interpolated for enthalpy, H_s. Thence isentropic velocity, V_{REAL}, is evaluated from Equation (14), the initial enthalpy H_t having been read from the tables.

Unfortunately, the calculated velocity was found to be extremely sensitive to error in the pressure-wise interpolation of entropy (path B → C in Figure 2) at the lower pressure ratios, as shown by the curve in Figure 3. In fact, all the standard numerical methods of interpolation* failed, as discussed in Appendix III, because the pressure intervals were too wide in the tables. Success was finally achieved with a pressure-wise interpolation by Real Air theory as described in Appendix III.

Real Air velocities were divided by Classic Air velocities, calculated as described in Section 4.4 to give the ratios, $V_{\text{REAL}}/V_{\text{CLASSIC}}$.

Finally the ratios of Real Air to Classic Air mass-flow intensity were found from:

$$\frac{(\rho V)_{\text{REAL}}}{(\rho V)_{\text{CLASSIC}}} = \frac{T_{s,\text{CLASSIC}}}{Z_s \times T_{s,\text{REAL}}} \times \frac{V_{\text{REAL}}}{V_{\text{CLASSIC}}} \tag{15}$$

since

$$\frac{\rho_{\text{REAL}}}{\rho_{\text{CLASSIC}}} = \frac{P_s}{ZRT_{s,\text{REAL}}} \Big/ \frac{P_s}{RT_{s,\text{CLASSIC}}} \tag{16}$$

---

*The 4-point Lagrangian interpolation, for which the Hilsenrath tables are said to be designed, was found to be numerically unstable and quite useless for the present calculations. Of the other methods investigated, a logarithmic transformation gave a good linear interpolation of S versus log P to within 5 digits in the last decimal place of entropy data (i.e. to 5 parts in 20 000) but this was not quite good enough for the present purposes.

4.3. *Ideal Air Isentropic Velocity and Mass-flow Intensity.*

Details of the calculation are given in Appendix IV for the computational path ABCDE illustrated in Figure 4.

The calculation is much simpler than for Real Air. Ideal Air enthalpy H^0 is independent of pressure, while a simple logarithmic pressure relationship exists for Ideal Air entropy S^0. In view of the basic simplicity of the calculation, and to take advantage of the greater precision of the tabulated values (S^0 data is given to 1 part of 200 000) it was decided to do a reverse interpolation of second degree for $T_{s,\mathrm{IDEAL}}$ (path D → E in Figure 4) instead of the linear reverse interpolation used in the Real Air program.

Having calculated enthalpy H_s^0 from $T_{s,\mathrm{IDEAL}}$, the Ideal Air isentropic velocity was found from Equation (14).

Ideal Air velocity was divided by Classic Air velocity, calculated as described in Section 4.4, to give the ratio, $V_{\mathrm{IDEAL}}/V_{\mathrm{CLASSIC}}$.

Finally, the ratio of Ideal Air to Classic Air mass flow intensity was found from:

$$\frac{(\rho V)_{\mathrm{IDEAL}}}{(\rho V)_{\mathrm{CLASSIC}}} = \frac{T_{s,\,\mathrm{CLASSIC}}}{T_{s,\,\mathrm{IDEAL}}} \times \frac{V_{\mathrm{IDEAL}}}{V_{\mathrm{CLASSIC}}} \tag{17}$$

since

$$\frac{\rho_{\mathrm{IDEAL}}}{\rho_{\mathrm{CLASSIC}}} = \frac{P_s}{R\,T_{s,\,\mathrm{IDEAL}}} \Big/ \frac{P_s}{R\,T_{s,\,\mathrm{CLASSIC}}} \tag{18}$$

4.4. *Classic Air Isentropic Velocity and Mass-flow Intensity.*

Isentropic velocity following expansion through the pressure ratio r is given by:

$$V_{\mathrm{CLASSIC}} = \left[\frac{\gamma R\,T_t M^2}{1+\dfrac{\gamma-1}{2}M^2} \right]^{\frac{1}{2}} \tag{19}$$

where

$$M^2 = \frac{2}{\gamma-1}\left(r^{\frac{\gamma-1}{\gamma}}-1\right) \tag{20}$$

and

$$r = P_t/P_s \tag{21}$$

while

$$\gamma = 1{\cdot}4 \text{ exactly for Classic Air.}$$

Equations (19) and (20) can be combined to give:

$$V_{\mathrm{CLASSIC}} = \left[\frac{2\gamma R}{\gamma-1}\,T_t\left(1-\left(\frac{1}{r}\right)^{\frac{\gamma-1}{\gamma}}\right) \right]^{\frac{1}{2}} \tag{22}$$

Mass-flow intensity is given by the product of velocity from Equation (22) with density from:

$$\begin{aligned}
\rho &= \frac{P_s}{R\,T_s} \\
&= \frac{P_t}{R\,T_t}\left(\frac{P_s}{P_t}\right)\left(\frac{T_t}{T_s}\right) \\
&= \frac{P_t}{R\,T_t}\,\frac{1}{r}.r^{\frac{\gamma-1}{\gamma}} \\
&= \frac{P_t}{R\,T_t}\left(\frac{1}{r}\right)^{\frac{1}{\gamma}}.
\end{aligned} \tag{23}$$

Hence

$$(\rho V)_{\text{CLASSIC}} = \left[\frac{2\gamma}{\gamma-1}\frac{P_t^2}{RT_t}\left(\frac{1}{r}\right)^{\frac{2}{\gamma}}\left\{1-\left(\frac{1}{r}\right)^{\frac{\gamma-1}{\gamma}}\right\}\right]^{\frac{1}{2}}. \tag{24}$$

Thus for Classic Air, the isentropic velocity and mass flow intensity can be calculated directly from Equations (22) and (24) for given nozzle inlet conditions P_t, T_t at any pressure ratio r, putting $\gamma = 1{\cdot}4$ exactly.

5. *Results.*

All the results presented in this Section 5 and shown in Figures 5, 6, 7, 8, 9, 10, and 11 are in the form of ratios of the properties of Real Air to those of Classic Air when the two fluids are expanded over *exactly the same pressure ratio*. This can be achieved in a 'flexible nozzle', but is strictly impossible in a 'fixed nozzle'. A full discussion is given in Section 6.

5.1. *Comparison of Classic Air with Ideal Air.*

Classic Air for which $\gamma = 1{\cdot}4$ exactly is a convenient reference fluid. Calculations of isentropic velocity V_{CLASSIC}, and mass-flow intensity $(\rho V)_{\text{CLASSIC}}$ are much simpler than their counterpart for Ideal Air, V_{IDEAL} and $(\rho V)_{\text{IDEAL}}$. So it is of practical interest to know the range over which Classic Air can be accepted as equivalent to Ideal Air.

Curves of $V_{\text{IDEAL}}/V_{\text{CLASSIC}}$ and $(\rho V)_{\text{IDEAL}}/(\rho V)_{\text{CLASSIC}}$ are plotted in Figures 5 and 6 against pressure ratio for various T_t levels above 300 deg K at a total pressure of 10 atm. It can be seen that if T_t is less than 400 deg K, both the velocity ratio and the mass-flow ratio remain within 0·1 per cent of unity.

Thus at the lower temperatures it is satisfactory to use Classic Air, instead of Ideal Air, as the basis for comparison with Real Air. Consequently, in this Report, properties of Real Air are published as ratios to the corresponding property of Classic Air. If the ratio of flow properties for Real Air/Ideal Air should be required, this can be found by the use of Figures 5 and 6.

5.2. *A Comparison of Calculation Methods for Real Air Mass Flow.*

Johnson[3] has published his results in the form of graphs of:

$$y = \frac{(\rho V)_{\text{REAL}}}{(\rho V)_{\text{IDEAL}}} - 1 \tag{25}$$

plotted against:

$$x = 1 - P_s/P_t$$

$$= 1 - \frac{1}{r} \tag{26}$$

at $T_t = 305{\cdot}55$ deg K, for P_t levels of 10, 40, 70 and 100 atm, for a range in pressure ratio r from 1 to 2.

Before comparing his results with those of the present calculations, two comments are necessary. Firstly, Johnson's label 'ideal' is synonymous with our label 'classic' for air with $\gamma = 1{\cdot}4$ exactly. Secondly, Johnson's equation for $(\rho V)_{\text{CLASSIC}}$ would be identical with our Equation (24) were it not for his inclusion of an 'arbitrary factor' (*sic*) Z_0 in the denominator. For purposes of comparison his Z_0 factor has been removed to give the curves of $(\rho V)_{\text{REAL}}/(\rho V)_{\text{CLASSIC}}$ plotted on Figure 7 for pressure ratio over the range from 1 to 2. Two inlet pressure levels are shown, 10 atm and 40 atm.

Results from the present calculations are also plotted on Figure 7 for pressure ratio r from 2 to 5. (At r less than 2 the present calculations are unreliable due to sensitivity to error in entropy data as shown on Figure 3). For r greater than 5 there is little further change in the level of the curves at least up to $r = 100$.

5.3. *Real Air/Classic Air Ratio of Isentropic Mass-flow Intensity.*

Ratios of $(\rho V)_{REAL}/(\rho V)_{CLASSIC}$ are plotted in Figure 8 for inlet-pressure levels of $P_t = 1, 4, 7$ and 10 atm over the range of pressure ratio from 2 to 10, all at a constant inlet temperature of $T_t = 290$ deg K. It is seen that the extent by which the ratio $(\rho V)_{REAL}/(\rho V)_{CLASSIC}$ increases from unity depends upon the inlet pressure level, but the effect is nearly independent of pressure ratio over the range from 5 to 100 (constant results for $r > 10$ are not shown). At inlet pressure of $P_t = 10$ atm the ratio $(\rho V)_{REAL}/(\rho V)_{CLASSIC}$ rises to between 0·6 per cent and 0·7 per cent in excess of unity (at the temperature of $T_t = 290$ deg K for which Figure 8 is drawn).

To show how the ratio $(\rho V)_{REAL}/(\rho V)_{CLASSIC}$ varies with inlet temperature, Figure 9 has been drawn for $T_t = 270, 300, 350$, and 400 deg K – all at a constant inlet pressure of $P_t = 10$ atm. As the inlet temperature increases from 270 to 400 deg K the ratio $(\rho V)_{REAL}/(\rho V)_{CLASSIC}$ decreases towards unity. At even higher temperatures, the ratio would pass through unity and decrease below it, but the use of Classic Air is unsuitable as a reference fluid for temperatures greater than about 400 deg K – *see* Section 5.1 and Figure 6.

5.4. *Real Air/Classic Air Ratio of Isentropic Velocity.*

Ratios of $V_{REAL}/V_{CLASSIC}$ are plotted in Figure 10 for inlet pressure levels of $P_t = 1, 4, 7$ and 10 atm over the range of pressure ratio from 2 to 10 – all at a constant inlet temperature of $T_t = 290$ deg K. Again, ratios of $V_{REAL}/V_{CLASSIC}$ are plotted in Figure 11 for inlet temperature levels of $T_t = 270, 300, 350$, and 400 deg K – all at a constant inlet pressure of $P_t = 10$ atm.

Effects of inlet pressure (at constant inlet temperature) or inlet temperature (at constant inlet pressure) are nearly independent of pressure ratio over the range from 2 to 100. (Results for $r > 10$ are not shown). The effect of increase of inlet pressure (Figure 10) is to cause the ratio $V_{REAL}/V_{CLASSIC}$ to fall away below unity – the opposite sense to the pressure effect on $(\rho V)_{REAL}/(\rho V)_{CLASSIC}$ in Section 5.3 and Figure 8.

At $P_t = 10$ atm, the ratio $V_{REAL}/V_{CLASSIC}$ is about 0·4 per cent less than unity at the inlet temperature of $T_t = 290$ deg K. As inlet temperature increases from 270 to 400 deg K with the same P_t (Figure 11) the ratio $V_{REAL}/V_{CLASSIC}$ rises to unity. At even higher inlet temperatures, the velocity ratio would increase above unity, but the use of Classic Air is unsuitable as a reference fluid for inlet temperatures greater than about 400 deg K – *see* Section 5.1. and Figure 5.

6. *Discussion.*

6.1. *Interpretation of Pressure Ratio.*

The results for $V_{IDEAL}/V_{CLASSIC}$, $(\rho V)_{IDEAL}/(\rho V)_{CLASSIC}$, $V_{REAL}/V_{CLASSIC}$ and $(\rho V)_{REAL}/(\rho V)_{CLASSIC}$ plotted in Figures 5 to 11 are ratios of one fluid property to another *at a common pressure ratio* (P_t/P_s). The velocity ratios in the Figures are identical with the isentropic specific thrust ratios when the fluids are imagined to expand fully within a 'flexible nozzle' so that P_s at exit is exactly equal to ambient pressure.

In Figure 10 for example the curve for $P_t = 10$ atm shows $V_{REAL}/V_{CLASSIC} = 0{\cdot}9960$ at the pressure ratio of $P_t/P_s = 10$. This velocity ratio would apply if Real Air, on the one hand, were to expand isentropically in a flexible convergent-divergent nozzle to $P_s = 1$ atm exactly at nozzle exit, while for comparison Classic Air were to expand isentropically to the same $P_s = 1$ atm at nozzle exit. The 'flexible nozzle' area ratio $(A^e/A^*)_{REAL}$ for Real Air would be slightly less than the area ratio $(A^e/A^*)_{CLASSIC}$ for Classic Air if the same P_s were to be achieved at nozzle exit. But if the two fluids were imagined to flow in fixed convergent-divergent nozzles of the same area ratio (as would be required for reference standards for 'fixed nozzle' isentropic efficiency) then the P_s at exit with Real Air would be slightly less than the P_s at exit with Classic Air. Figure 12 has been drawn to illustrate these distinctions using inlet conditions of $P_t = 10$ atm, $T_t = 290$ deg K, as an example.

Application of the results for flow in 'fixed nozzles' is discussed in the following sections.

6.2. *Choking Mass Flow in Fixed Convergent Nozzles.*

Mass flow intensities (ρV) calculated for Real Air and for Classic Air are shown in Figure 13 for inlet conditions $P_t = 10$ atm, $T_t = 290$ deg K, plotted separately against pressure ratio P_t/P_s. The position and shape of the Classic Air curve can be relied upon quite precisely and gives a choking mass flow of:

$$(\rho V)^*_{\text{CLASSIC}} = 2404{\cdot}4 \text{ kg/s.m}^2 \tag{27}$$

at the critical pressure ratio of:

$$(P_t/P_s)^*_{\text{CLASSIC}} = 1{\cdot}893. \tag{28}$$

There is less certainty about the Real Air curve, particularly at these lower pressure ratios (*see* sensitivity in Figure 3) and so we cannot pick off the exact choking pressure ratio from Figure 12. What we can say for Real Air is that, approximately

$$(P_t/P_s)^*_{\text{REAL}} \simeq 1{\cdot}90 \tag{29}$$

and

$$(\rho V)^*_{\text{REAL}} \simeq 2414{\cdot}5 \text{ kg/s.m}^2. \tag{30}$$

Hence for $P_t = 10$ atm, $T_t = 290$ deg K, we have:

$$\frac{(\rho V)^*_{\text{REAL}}}{(\rho V)^*_{\text{CLASSIC}}} = \frac{2414{\cdot}5}{2404{\cdot}4} = 1{\cdot}0042. \tag{31}$$

Now for a common pressure ratio of, say, $P_t/P_s = 1{\cdot}9$ for both Real Air and Classic Air we would have from Figure 13:

$$\frac{(\rho V)_{\text{REAL}}}{(\rho V)_{\text{CLASSIC}}} = \frac{2414{\cdot}5}{2404{\cdot}4} = 1{\cdot}0042. \tag{32}$$

At any other nearby common pressure ratio, say $P_t/P_s = 2{\cdot}0$, for both Real Air and Classic Air we would have from Figure 13:

$$\frac{(\rho V)_{\text{REAL}}}{(\rho V)_{\text{CLASSIC}}} = \frac{2410{\cdot}1}{2400{\cdot}1} = 1{\cdot}0042. \tag{33}$$

This latter result could have been read off the appropriate curve plotted on either Figure 7 or Figure 8.

Comparing the exact Equation (31) with (32) or (33) it would seem to be sufficiently precise to take results for $(\rho V)_{\text{REAL}}/(\rho V)_{\text{CLASSIC}}$ at any common pressure ratio near choking for both Real Air and Classic Air in a fixed convergent nozzle. A sufficiently accurate measurement of actual mass flow of Real Air in a choked convergent nozzle is then:

$$Q_{\text{REAL}} = \left[\frac{(\rho V)_{\text{REAL}}}{(\rho V)_{\text{CLASSIC}}}\right]_{\substack{\text{near}\\ \text{choking}}} \times (\rho V)^*_{\text{CLASSIC}} \times A^* \tag{34}$$

where the first factor on the R.H.S. of Equation (34) can be read off the curves of $(\rho V)_{\text{REAL}}/(\rho V)_{\text{CLASSIC}}$ that are plotted against common pressure ratio (e.g., Figures 7, 8, 9). The second factor $(\rho V)^*_{\text{CLASSIC}}$ can be calculated from Equation (24), or in any other convenient way.

6.3. *Mass-flow Intensities in Fixed Convergent-Divergent Nozzles.*

Consider a convergent-divergent nozzle of fixed area ratio A^e/A^* through which Real Air flows with given inlet conditions P_t, T_t. Then by the continuity equation:

$$\rho VA = \text{constant} = (\rho VA)^* \tag{35}$$

we have for the mass-flow intensity at nozzle exit:

$$(\rho V)^e_{\text{REAL}} = (\rho V)^*_{\text{REAL}} \frac{A^*}{A^e}. \tag{36}$$

Similarly, for Classic Air flowing through the same 'fixed nozzle' we have:

$$(\rho V)^e_{\text{CLASSIC}} = (\rho V)^*_{\text{CLASSIC}} \frac{A^*}{A^e} \tag{37}$$

Therefore from Equations (36) and (37):

$$\frac{(\rho V)^e_{\text{REAL}}}{(\rho V)^e_{\text{CLASSIC}}} = \frac{(\rho V)^*_{\text{REAL}}}{(\rho V)^*_{\text{CLASSIC}}} \tag{38}$$

Hence the ratio of Real Air/Classic Air mass-flow intensity in the 'fixed nozzle' exit plane (or in any other plane within the 'fixed nozzle') is independent of pressure ratio and of area ratio, when the two fluids are imagined to flow in turn through the same fixed choked nozzle.

It should be carefully noted that this phenomenon of a constant ratio of $(\rho V)_{\text{REAL}}/(\rho V)_{\text{CLASSIC}}$ applies only to flow of the two fluids through a *fixed* convergent-divergent nozzle. It does not hold when the two fluids are imagined to expand through 'flexible nozzles' over a given pressure ratio, as can be seen for example from Figure 7, or as illustrated in Figure 12.

It has already been shown in Section 6.2 that the ratio $(\rho V)^*_{\text{REAL}}/(\rho V)^*_{\text{CLASSIC}}$ can be read from curves that are plotted against a common pressure ratio, such as Figures 7, 8, or 9. The curves should be read in the neighbourhood of $r = 2{\cdot}0$ to give the appopriate value for Equation (38) for the particular inlet conditions of P_t, T_t. For example, from Figure 7 or 8 we have:

$$\frac{(\rho V)^*_{\text{REAL}}}{(\rho V)^*_{\text{CLASSIC}}} = 1{\cdot}0042 \tag{39}$$

for $P_t = 10$ atm, $T_t = 290$ deg K. And this value remains constant at every plane within a 'fixed nozzle' of any area ratio, operating at any pressure ratio greater than the choking value. (Since we are considering uniform isentropic flow, the possibility of flow break-away from the nozzle walls does not arise.)

6.4. *Thrust Ratio with Fixed Convergent-Divergent Nozzles.*

It has been pointed out in Section 6.1 that it is impossible to operate a convergent-divergent nozzle of fixed area ratio with exactly the same static pressure in the exit plane for both Real Air and Classic Air. For given inlet conditions, P_t and T_t, the static pressure at exit with Real Air, $P^e_{s,\text{REAL}}$, will be less than that with Classic Air, $P^e_{s,\text{CLASSIC}}$. Nevertheless one feels (and hopes) intuitively that the curves of Real Air/ Classic Air isentropic velocity ratio, $V_{\text{REAL}}/V_{\text{CLASSIC}}$, might still apply approximately to the case of the 'fixed nozzle' with area ratio A^e/A^* designed to suit one of the two fluids. Such a belief is examined below.

Now with a 'flexible nozzle' the ratio of Real Air/Classic Air isentropic thrust for full expansion to the common static pressure:

$$P^e_{s,\text{REAL}} = P^e_{s,\text{CLASSIC}} = P_\infty \tag{40}$$

is given by the velocity ratio $V_{\text{REAL}}/V_{\text{CLASSIC}}$ read from the curves in Figures 10 or 11.

With a 'fixed nozzle', the area ratio

$$\frac{A^e}{A^*} = \frac{(\rho V)^*_{\text{REAL}}}{(\rho V)^e_{\text{REAL}}} \tag{41}$$

would give correct expansion of Real Air to:

$$P^e_{s,\text{REAL}} = P_\infty \tag{42}$$

at exit.

The performance of Classic Air in this 'fixed nozzle' is calculated as follows. For the area ratio given by Equation (41), the exit Mach number for Classic Air can be found from:

$$\frac{A^e}{A^*} = \frac{1}{M}\left[\frac{2}{\gamma+1} + \frac{\gamma-1}{\gamma+1}M^2\right]^{\frac{\gamma+1}{2(\gamma-1)}} \tag{43}$$

solving for M by iteration. Thence the corresponding pressure ratio and velocity can be calculated directly from:

$$\left(\frac{P_t}{P_s}\right)_{\text{CLASSIC}} = \left[1 + \frac{\gamma-1}{2}M^2\right]^{\frac{\gamma}{\gamma-1}} \tag{44}$$

and

$$V_{\text{CLASSIC}} = (\gamma R\, T_t)^{\frac{1}{2}} \frac{M}{\left[1 + \frac{\gamma-1}{2}M^2\right]^{\frac{1}{2}}}. \tag{45}$$

These calculations have been made for the inlet conditions $P_t = 10$ atm, $T_t = 290$ deg K, and some of the results are shown on Figure 14. From the Figure it can be seen that if Classic Air were to flow through a series of 'fixed nozzles' with area ratios designed to suit Real Air (i.e. A^e/A^* equal to 1·70357, 1·81734, and 1·92563 for $(P_t/P_s)_{\text{REAL}}$ equal to 8, 9, and 10 in Figure 13) then the ratio of Real Air/Classic Air isentropic velocity would be approximately:

$$\left[\frac{V_{\text{REAL}}}{V_{\text{CLASSIC}}}\right]_{\text{FIXED NOZ}} \simeq 0{\cdot}9965 \tag{46}$$

in each case. The corresponding velocity ratios when expanding through a 'flexible nozzle' over a common pressure ratio for the two fluids would be approximately:

$$\left[\frac{V_{\text{REAL}}}{V_{\text{CLASSIC}}}\right]_{\text{FLEXIBLE NOZ}} \simeq 0{\cdot}9960 \tag{47}$$

in each case.

It was found that over the whole range of pressure ratio from $r = 2$ to 100, the 'fixed nozzle' Real Air/Classic Air velocity ratio was only about 0·05 per cent higher than the 'flexible nozzle' velocity ratio.

Furthermore, the slight excess of static pressure at nozzle exit with Classic Air in the 'fixed nozzle' would add a little pressure-thrust to help redress the balance of velocity-thrust in the Real Air/Classic Air isentropic velocity ratio.

Hence it would seem that the curves of $V_{REAL}/V_{CLASSIC}$ in Figures 10 and 11, although plotted for a common pressure ratio for the two fluids such as would be achieved with a 'flexible nozzle', are, nevertheless, a good approximation to the Real Air/Classic Air velocity ratio in a series of 'fixed nozzles' designed to suit only one of the fluids.

Acknowledgements.

The author gratefully acknowledges the help of Veronica Pinker who was responsible for most of the computer programming. Thanks are also due to Doris Frampton who came in to help with the later calculations.

LIST OF SYMBOLS

Symbol	Description	Units	
		Fundamental mechanical ft.lb.s.	m.k.s.
a	Mean slope of compressibility data $= \frac{Z_2 - Z_1}{P_2 - P_1}$	1/atm or, ft^2/pdl	1/atm or, m^2/N
A	Flow area	ft^2	m^2
b	Mean slope of $\left(\frac{\partial Z}{\partial T}\right)$ $= \frac{\left(\frac{\partial Z}{\partial T}\right)_2 - \left(\frac{\partial Z}{\partial T}\right)_1}{P_2 - P_1}$	1/atm deg K or, ft^2/pdl deg K	1/atm deg K or, m^2/N deg K
C_p	Specific heat at constant pressure	ft.pdl/lb. deg K	J/kg. deg K
C_v	Specific heat at constant volume	ft.pdl/lb. deg K	J/kg. deg K
E	Internal energy	ft.pdl/lb	J/kg
f	General function	as appropriate	as appropriate
h	Tabular interval $= x_1 - x_0$	as appropriate	as appropriate
H	Enthalpy	ft.pdl/lb	J/kg
K	Kinetic energy	ft.pdl/lb	J/kg
l	Length of flow element	ft	m
M	Mach number	N.D.	N.D.
p	Relative interval of interpolation $= \frac{x_p - x_0}{h}$		
P	Pressure	pdl/ft^2 or, atm	N/m^2 or, atm
Q	Mass-flow rate	lb/s	kg/s
r	Pressure ratio $= P_t/P_s$	N.D.	N.D.
R	Gas constant = 287·041 J/kg deg K for air	ft.pdl/lb. deg K	J/kg. deg K
S	Entropy	ft.pdl/lb. deg K	J/kg. deg K
T	Temperature	deg K	deg K
v	Specific volume $= 1/\rho$	ft^3/lb	m^3/kg
V	Velocity	ft/s	m/s
W	Work	ft.pdl/lb	J/kg

LIST OF SYMBOLS (contd.)

Symbol	Description	Units	
		Fundamental mechanical ft.lb.s.	m.k.s.
x	either (i) length of duct or (ii) independent tabular variable	ft as appropriate	m as appropriate
X_G	Gross (gauge) thrust	pdl	N
Z	Compressibility factor $= \frac{P}{\rho R T}$	N.D.	N.D.
γ	Ratio of specific heats $= \frac{C_p}{C_v}$	N.D.	N.D.
δ	First difference of tabulated function (*see* Table 1, Appendix III)	as appropriate	as appropriate
δ^2	Second difference (*see* Table 2, Appendix IV)	as appropriate	as appropriate
ρ	Density	lb/ft^3	kg/m^3
[ ]	Subject of mathematical operator, usually $\delta[\ ]$		

LIST OF SYMBOLS (contd.)

Symbol	Description
Suffices	
CLASSIC IDEAL REAL	} *see* Section 2.1, 2.2, 2.3.
n	Pressure level between tabulated P_1 and P_2
nom	(i) necessarily at T_{nom}, a selected temperature near to T_s (ii) but also at pressure P_s in the case of S_{nom}, H_{nom}, Z_{nom}
o	either (i) at standard temperature $T_0 = 273{\cdot}16$ deg K or (ii) at 0 deg K in the case of E_0^0
is	Isentropic
s	Static
t	Total, i.e., stagnation
∞	Ambient
1,2	Tabulated data points
$\frac{1}{2}, -\frac{1}{2}$ $1\frac{1}{2}, -1\frac{1}{2}$	} Tabulated levels Defined by Tables 1 and 2
Indices	
e	Nozzle exit plane
o	Ideal Air
$'$	Redefined data point at temperature 10 deg less than previously
*	Choking, i.e. $M = 1$

LIST OF REFERENCES

No.	*Author(s)*	*Title, etc.*
1	J. C. Ascough	Real Air effects in propelling nozzles. Unpublished work at N.G.T.E. February 1964.
2	J. Hilsenrath et al	*Tables of thermodynamic and transport properties of air, argon, carbon dioxide, carbon monoxide, hydrogen, nitrogen, oxygen and steam.* Pergamon Press. 1960.
3	R. C. Johnson	Calculations of Real Gas effects in flow through critical-flow nozzles. Trans. A.S.M.E., Series D, Vol. 86. September 1964.
4	O. A. Hougen and K. M. Watson	*Chemical process principles Part Two – thermodynamics.* John Wiley & Sons / Chapman and Hall } 7th printing 1955.

APPENDIX I

Basic Principles in Propelling-nozzle Performance.

In Section 4.1 the specific thrust of a propelling nozzle operating at the D.P.R. was shown to be:

$$\left[\frac{X_G}{Q\sqrt{T_t}}\right]_{\text{DPR}} = \frac{V^e}{\sqrt{T_t}} \quad \text{as Equation (11)}$$

or

$$\left[\frac{X_G}{Q}\right]_{\text{DPR}} = V^e \tag{I.01}$$

An expression for this velocity in terms of an enthalpy difference is derived as follows. Applying the principle of the conservation of energy to the flow within a duct of changing cross-section, we have: 'The increase in kinetic energy and internal energy of an element of gas is equal to the net work done on the gas by the changing pressure forces (in the absence of friction)'. Referring to the lower diagram in Figure 1, we imagine the expansion, due to translation dx, to occur in two stages, thus:

Stage 1 = Translation without change of volume v, in which there is a net pressure difference $\left(l\frac{dP_s}{dx}\right)$ on the element. This pressure difference is constant even though the pressure level changes to (P_s+dP_s). Hence we have for the work done on the element:

$$dW_1 = \left(-l\frac{dP_s}{dx}\right) A\,dx \tag{I.02}$$

$$= -(lA)\ dP_s$$

$$= -v\,dP_s \tag{I.03}$$

Stage 2 = Pure expansion at constant pressure without translation. Hence we have for the work done on the element:

$$dW_2 = -(P_s+dP_s)\,dv \tag{I.04}$$

$$= -P_s dv, \text{ to first order.} \tag{I.05}$$

Now, the change in kinetic energy of unit mass of the gas is:

$$dK = d\left(\tfrac{1}{2}V^2\right)$$

$$= V\,dV. \tag{I.06}$$

Then, denoting the change in internal energy as dE, it follows from the conservation of energy that:

$$dK+dE = dW_1+dW_2 \tag{I.07}$$

therefore substituing from Equations (I.03), (I.05), (I.06) in (I.07):

$$V\,dV+dE = -vdP_s-P_s dv \tag{I.08}$$

$$= -d(P_s v) \tag{I.09}$$

i.e.

$$V\,dV + d(P_s v) + dE = 0. \tag{I.10}$$

But a change in enthalpy is defined as:

$$dH_s = d(P_s v) + dE \tag{I.11}$$

therefore Equations (I.10), (I.11):

$$V\,dV + dH_s = 0. \tag{I.12}$$

Integrating Equation (I.12):

$$\frac{V_2}{2} + H_s = \text{constant} = H_t \tag{I.13}$$

i.e.

$$V = \sqrt{2(H_t - H_s)}. \tag{I.14}$$

Hence, the isentropic specific gross thrust for full expansion is found by substituting for V from Equation (I.14) into Equation (I.01).

The equations established above can apply generally to the isentropic expansion of either Classic Air, Ideal Air, or Real Air. The main problem to be solved in the present work is to calculate values of enthalpy, H_s, following an isentropic expansion of Real Air, in order that isentropic velocity may be found from Equation (I.14).

APPENDIX II

A Calculation of Real Air Entropy.

An essential step in the calculation in Appendix III is the interpolation at constant temperature T_{nom} of a value for entropy S_{nom} at pressure P_s between two tabulated levels S_1 at P_1 and S_2 at P_2 (path B → C in Figure 2). Unfortunately all the standard numerical methods for interpolation failed because the pressure intervals were too wide in the tables. So it was necessary to fall back on Real Air theory as developed below. (The basic thermodynamics can be found in Hougen and Watson[4].)

Since entropy is a point function it can be expressed by the exact differential equation:

$$dS = \left(\frac{\partial S}{\partial T}\right)_P dT + \left(\frac{\partial S}{\partial P}\right)_T dP. \tag{II.01}$$

But

$$\left(\frac{\partial S}{\partial T}\right)_P = \frac{C_p}{T} \tag{II.02}$$

and

$$\left(\frac{\partial S}{\partial P}\right)_T = -\left(\frac{\partial v}{\partial T}\right)_P. \tag{II.03}$$

Now from

$$Pv = ZRT \tag{II.04}$$

or

$$v = \frac{ZRT}{P} \tag{II.05}$$

we obtain

$$\left(\frac{\partial v}{\partial T}\right)_P = \frac{ZR}{P} + \frac{RT}{P}\left(\frac{\partial Z}{\partial T}\right)_P. \tag{II.06}$$

Hence, substituting in Equation (II.01) from Equations (II.02), (II.03), (II.06)

$$dS = \frac{C_p dT}{T} - \left[\frac{RZ}{P} + \frac{RT}{P}\left(\frac{\partial Z}{\partial T}\right)_P\right] dP \tag{II.07}$$

i.e.

$$\frac{dS}{R} = \frac{C_p}{R}\frac{dT}{T} - \left[Z + T\left(\frac{\partial Z}{\partial T}\right)_P\right]\frac{dP}{P} \tag{II.08}$$

Equation (II.08) may be integrated to give a change in entropy corresponding to a change in pressure at constant temperature T_{nom}. Thus for a change in pressure from tabulated level P_1 to any other pressure P_n, within the tabular interval P_1 to P_2, we have:

$$\frac{S_n - S_1}{R} = -\int_{P_1}^{P_n}\left[Z + T_{nom}\left(\frac{\partial Z}{\partial T}\right)_P\right]\frac{dP}{P}. \tag{II.09}$$

Consider the first term on R.H.S. of Equation (II.09), $\int_{P_1}^{P_n} Z\frac{dP}{P}$. An examination of Hilsenrath's tables shows that Z is a nearly linear function of P, i.e.

$$Z = Z_1 + a(P - P_1) \tag{II.10}$$

where

$$a = \frac{Z_2 - Z_1}{P_2 - P_1}. \tag{II.11}$$

(The mean slope a between P_1 and P_2 is in fact negative.) Hence we have for the first term an R.H.S. of Equation (II.09):

$$\int_{P_1}^{P_n} Z \frac{dP}{P} = \int_{P_1}^{P_n} \left[Z_1 + a(P - P_1) \right] \frac{dP}{P} \tag{II.12}$$

$$= (Z_1 - aP_1) \ln\left(\frac{P_n}{P_1}\right) + a(P_n - P_1). \tag{II.13}$$

Next consider the second term on R.H.S. of Equation (II.09), i.e. $\int_{P_1}^{P_n} T_{\text{nom}} \left(\frac{\partial Z}{\partial T}\right)_P \frac{dP}{P}$. The partial derivative $\left(\frac{\partial Z}{\partial T}\right)_P$ is required as the instantaneous derivative at the temperature T_{nom}, i.e. *not* a mean slope between T_{nom} and ($T_{\text{nom}} + 10$ deg) given by $\delta_{\frac{1}{2}} \left[Z \right]$. Furthermore, $\left(\frac{\partial Z}{\partial T}\right)_P$ is required at a pressure P_n that is not tabulated. Hence we have, first for a tabulated pressure level:

$$\left(\frac{\partial Z}{\partial T}\right) = \frac{1}{h} \times (\text{mean value of } \delta_{\frac{1}{2}} \text{ and } \delta_{-\frac{1}{2}}) \tag{II.14}$$

$$= \frac{1}{10} \times \frac{1}{2} \left(\delta_{\frac{1}{2}} \left[Z \right] + \delta_{-\frac{1}{2}} \left[Z \right] \right). \tag{II.15}$$

Having calculated $\left(\frac{\partial Z}{\partial T}\right)_{P_1}$ and $\left(\frac{\partial Z}{\partial T}\right)_{P_2}$ for the tabulated pressure levels P_1 and P_2, by means of Equation (II.15), we then obtain $\left(\frac{\partial Z}{\partial T}\right)_P$ by linear interpolation. Thus:

$$\left(\frac{\partial Z}{\partial T}\right)_P = \left(\frac{\partial Z}{\partial T}\right)_{P_1} + b(P - P_1) \tag{II.16}$$

where

$$b = \frac{\left(\frac{\partial Z}{\partial T}\right)_{P_2} - \left(\frac{\partial Z}{\partial T}\right)_{P_1}}{P_2 - P_1}. \tag{II.17}$$

Hence,

$$\int_{P_1}^{P_n} T_{\text{nom}} \left(\frac{\partial Z}{\partial T}\right)_P \frac{dP}{P} = T_{\text{nom}} \int_{P_1}^{P_n} \left[\left(\frac{\partial Z}{\partial T}\right)_{P_1} + b(P - P_1) \right] \frac{dP}{P} \tag{II.18}$$

$$= T_{\text{nom}} \left[\left(\left(\frac{\partial Z}{\partial T} \right)_{P_1} - bP_1 \right) ln\, P + bP \right]_{P_1}^{P_n} \tag{II.19}$$

$$= T_{\text{nom}} \left[\left(\left(\frac{\partial Z}{\partial T} \right)_{P_1} - bP_1 \right) ln \left(\frac{P_n}{P_1} \right) + b\,(P_n - P_1) \right] . \tag{II.20}$$

Finally, substituting from Equation (II.13), (II.20) into (II.09):

$$\frac{S_n - S_1}{R} = - \left\{ \left[Z_1 + T_{\text{nom}} \left(\frac{\partial Z}{\partial T} \right)_{P_1} - (a + b\,T_{\text{nom}})\, P_1 \right] ln \left(\frac{P_n}{P_1} \right) + (a + b\,T_{\text{nom}})\,(P_n - P_1) \right\} \tag{II.21}$$

Equation (II.21) was used successfully for a pressure-wise 'interpolation', as Equation (III.06) in Appendix III, after all the usual numerical methods interpolations had failed.

APPENDIX III

Calculation Procedure for V_{REAL} *and* $(\rho V)_{\text{REAL}}$

An electronic computer program has been written for the calculations of the computational path illustrated in Figure 2 and described below.

Entropy and enthalpy data are tabulated by Hilsenrath in non-dimensional form as S/R and $(H-E_0^0)/RT_0$. To avoid unnecessary complication, the Notation S and H is used in this Appendix to signify these non-dimensional quantities. Only at Equation (III.20) and after, will dimensional form be used.

Path A → B, (*preliminary selection of data*).

For each given value of T_t and r, calculate

$$T_{s\,\text{CLASSIC}} = T_t/r^{\frac{\gamma-1}{\gamma}} \tag{III.01}$$

for

$$\gamma = 1{\cdot}4.$$

Select T_{nom} = nearest temperature to $T_{s,\text{CLASSIC}}$ in Hilsenrath's tables (steps of 10 deg C).

For each given value of P_t and r calculate:

$$P_s = P_t/r. \tag{III.02}$$

Select P_1, P_2 = nearest pressure levels, below and above P_s, in Hilsenrath's tables at temperature T_{nom}. Extract the following data from Hilsenrath's tables:

$$Z_1\ Z_2\ \delta_{\frac{1}{2}}[Z_1]\ \delta_{\frac{1}{2}}[Z_2]\ \delta_{-\frac{1}{2}}[Z_1]\ \delta_{-\frac{1}{2}}[Z_2]$$

$$S_1\ S_2\ \delta_{\frac{1}{2}}[S_1]\ \delta_{\frac{1}{2}}[S_2]\ \delta_{-\frac{1}{2}}[S_1]\ \delta_{-\frac{1}{2}}[S_2]$$

$$H_1\ H_2\ \delta_{\frac{1}{2}}[H_1]\ \delta_{\frac{1}{2}}[H_2]\ \delta_{-\frac{1}{2}}[H_1]\ \delta_{-\frac{1}{2}}[H_2]$$

where the δ's are tabulated first differences for *changes in temperature* from T_{nom}, at constant pressure. The Notation for δ is illustrated in the following Table, using Z at constant pressure as an example:

TABLE 1

$x = T$	$f[x] = Z$	$\delta[Z]$
		$\delta_{-1\frac{1}{2}} = Z_{-1} - Z_{-2}$
x_{-1}	Z_{-1}	
		$\delta_{-\frac{1}{2}} = Z_0 - Z_{-1}$
$T_{\text{nom}} = x_0$	Z_0	
		$\delta_{\frac{1}{2}} = Z_1 - Z_0$
x_1	Z_1	
		$\delta_{1\frac{1}{2}} = Z_2 - Z_1$
x_2	Z_2	

(N.B. The suffices $_1$ and $_2$ for data points defined in Figure 2 are meant to be distinct from the suffices in Table 1.)

The tabular interval used throughout Hilsenrath's tables is:

$$h = x_2 - x_1 = x_1 - x_0, \text{ etc.}$$

$$= 10 \text{ deg C.} \tag{III.03}$$

Path B → C.

Much difficulty was experienced in the early attempts to interpolate for S_{nom} at constant temperature T_{nom} between the tabulated S_1, S_2. Very high precision was required because of the sensitivity of the final V_{REAL} to error in S. It was found that the 4-point Lagrangian interpolation recommended in the Hilsenrath tables was numerically unstable. Several other interpolation methods were tried, *viz*: quadratic fit to 3 tabular points, quadratic fit by least squares to 4 tabular points, Fourier series fit to 4 tabular points, either linear 2-point or Langrangian 4-point fit to S versus log P. All of these were inadequate, although the S versus log P transformation came within 5 digits of the last decimal place of S, or 5 parts in 20 000 which was very near to the required precision. Finally, it was decided to interpolate by the theoretical relationship established as Equation (II.21) of Appendix II, putting:

$$P_n = P_s \tag{III.04}$$

and

$$S_n = S_{nom}. \tag{III.05}$$

Thus, committing the gas constant R to memory:

$$S_{nom} = S_1 - \left\{ \left[Z_1 + T_{nom} \left(\frac{\partial Z}{\partial T} \right)_{P_1} - (a + b\,T_{nom})\,P_1 \right] ln \frac{P_s}{P_1} + (a + b\,T_{nom})\,(P_s - P_1) \right\} \tag{III.06}$$

where

$$a = \frac{Z_2 - Z_1}{P_2 - P_1} \tag{III.07}$$

and

$$b = \frac{\left(\frac{\partial Z}{\partial T} \right)_{P_2} - \left(\frac{\partial Z}{\partial T} \right)_{P_1}}{P_2 - P_1} \tag{III.08}$$

and

$$\left(\frac{\partial Z}{\partial T} \right)_P = \frac{1}{10} \times \frac{1}{2} \left(\delta_{-\frac{1}{2}} \left[Z \right]_P + \delta_{\frac{1}{2}} \left[Z \right]_P \right) \tag{III.09}$$

Equations (III.06) through to (III.09) make use of numerical methods of finite differences, neglecting differences higher than the first. It is believed that the resulting value of S_{nom} is precise within 1 digit in the last decimal place of the tabulated S_1 or S_2 data, i.e., within 1 part in 20 000.

Interpolations at constant temperature T_{nom} for H_{nom} and Z_{nom} were found to be adequate by linear 2-point methods, *viz*:

$$H_{nom} = H_1 + \frac{(H_2 - H_1)}{(P_2 - P_1)} \times (P_s - P_1) \tag{III.10}$$

and

$$Z_{nom} = Z_1 + \frac{(Z_2 - Z_1)}{(P_2 - P_1)} \times (P_s - P_1) \tag{III.11}$$

The procedure described above for the interpolation path B → C in Figure 2 would apply with the same intrinsic precision for the path B′ → C. Values of H_{nom}, Z_{nom} would be identical by either path, but slight numerical discrepancies arise in S_{nom} from inconsistencies in the tabulated S_1, S_2 (e.g. effects of rounding off error in the last decimal place are noticeable).

Path C → D.

We need to find the temperature $T_{s,\mathrm{REAL}}$, at constant pressure P_s, at which the entropy S_s is equal to the initial entropy S_t, i.e. an isentropic process. This is achieved by reverse linear interpolation. Thus, in the standard notation of numerical methods, neglecting terms in higher differences than the first:

$$f_p = f_0 + p\delta_{\frac{1}{2}} + \ldots\ldots \tag{III.12}$$

For case (a), $T_s > T_{\mathrm{nom}}$, Equation (III.12) becomes:

$$S_t = S_{\mathrm{nom}} + \frac{T_s - T_{\mathrm{nom}}}{10} \times \delta_{\frac{1}{2}}[S]_{P_s} \tag{III.13}$$

therefore

$$T_s = T_{\mathrm{nom}} + \frac{10}{\delta_{\frac{1}{2}}[S]_{P_s}}(S_t - S_{\mathrm{nom}}). \tag{III.14}$$

For case (b), $T_s < T_{\mathrm{nom}}$,

$$T_s = T_{\mathrm{nom}} - \frac{10}{\delta_{-\frac{1}{2}}[S]_{P_s}}(S_{\mathrm{nom}} - S_t) \tag{III.15}$$

Here, the first differences $\delta_{\frac{1}{2}}[S]_{P_s}$ and $\delta_{-\frac{1}{2}}[S]_{P_s}$ are required at the pressure P_s (which is not tabulated) and are therefore calculated from the tabulated first differences $\delta_{\frac{1}{2}}[S]_{P_1}$, $\delta_{\frac{1}{2}}[S]_{P_2}$ and $\delta_{-\frac{1}{2}}[S]_{P_1}$, $\delta_{-\frac{1}{2}}[S]_{P_2}$ by linear interpolation.

Having obtained the temperature T_s by Equation (III.14) for case (a), or Equation (III.15) for case (b) we proceed to calculate H_s and Z_s by linear interpolation. Thus for case (a):

$$H_s = H_{\mathrm{nom}} + \frac{\delta_{\frac{1}{2}}[H]_{P_s}}{10}(T_s - T_{\mathrm{nom}}) \tag{III.16}$$

and

$$Z_s = Z_{\mathrm{nom}} + \frac{\delta_{\frac{1}{2}}[Z]_{P_s}}{10}(T_s - T_{\mathrm{nom}}) \tag{III.17}$$

or for case (b):

$$H_s = H_{\mathrm{nom}} - \frac{\delta_{-\frac{1}{2}}[H]_{P_s}}{10}(T_{\mathrm{nom}} - T_s) \tag{III.18}$$

and

$$Z_s = Z_{\mathrm{nom}} - \frac{\delta_{-\frac{1}{2}}[Z]_{P_s}}{10}(T_{\mathrm{nom}} - T_s). \tag{III.19}$$

As before, the first differences $\delta_{\frac{1}{2}}[\,]_{P_s}$, $\delta_{-\frac{1}{2}}[\,]_{P_s}$ at pressure P_s which is not tabulated, are calculated from the first differences tabulated at pressures P_1 and P_2 by linear interpolation.

Having evaluated the properties at point 'D' in Figure 2, the Real Air velocity can be calculated from Equation (I.14) of Appendix I:

$$V_{\mathrm{REAL}} = \sqrt{2(H_t - H_s)}$$

However, this equation is in dimensional form and would give velocity in units of $[m/s]$ if the enthalpies were given in units of $[J/kg]$. But the calculations up to this stage in this Appendix have used non-dimensional enthalpy $(H - E_0^0)/RT_0$ as tabulated by Hilsenrath, which had been simplified to the Notation 'H'. Hence, putting:

$$R = 287{\cdot}041\ J/kg.\ \text{deg K} \tag{III.20}$$

and

$$T_0 = 273{\cdot}16\ \text{deg K} \tag{III.21}$$

we need to multiply the enthalpy difference in Equation (I.19) by the factor:

$$RT_0 = 78408{\cdot}0\ J/kg. \tag{III.22}$$

Thus we obtain the practical equation for isentropic Real Air velocity:

$$V_{\text{REAL}} = \sqrt{156816\,(H_t - H_s)}\ m/s \tag{III.23}$$

where both H_t and H_s are non-dimensional values.

Classic Air isentropic velocity is calculated from:

$$V_{\text{CLASSIC}} = \left[\frac{\gamma R\, T_t\, M^2}{1+\dfrac{\gamma-1}{2}M^2}\right]^{\frac{1}{2}}\ m/s \tag{III.24}$$

where

$$M^2 = \frac{2}{\gamma-1}\left(r^{\frac{\gamma-1}{\gamma}} - 1\right) \tag{III.25}$$

putting

$$\gamma = 1{\cdot}4.$$

The Real Air/Classic Air isentropic velocity ratio, $V_{\text{REAL}}/V_{\text{CLASSIC}}$ can be obtained from Equations (III.23) and (III.24).

The Real Air/Classic Air isentropic mass flow intensity ratio can be obtained by substituting from Equations (III.01), (III.14) or (III.15), (III.17) or (III.19), (III.23) and (III.24) in the following:

$$\frac{(\rho V)_{\text{REAL}}}{(\rho V)_{\text{CLASSIC}}} = \left(\frac{T_{s,\text{CLASSIC}}}{Z_s \times T_{s,\text{REAL}}}\right) \times \left(\frac{V_{\text{REAL}}}{V_{\text{CLASSIC}}}\right) \tag{III.26}$$

APPENDIX IV

Calculation Procedure for V_{IDEAL} *and* $(\rho V)_{\text{IDEAL}}$.

An electronic computer program has been written for the calculations of the computational path illustrated in Figure 4 and described below.

Ideal Air entropy and enthalpy data are tabulated by Hilsenrath in non-dimensional form, as S^0/R for the standard pressure of 1 atm, and $(H^0 - E_0^0)/RT_0$ which is independent of pressure. For the most of this Appendix, the Notation $S^0_{1\text{ atm}}$ and H^0 are used to signify these non-dimensional quantities.

Points B and C (preliminary selection of data).

For each given value of T_t and r, calculate as Equation (III.01).

$$T_{s,\text{CLASSIC}} = T_t/r^{\frac{\gamma-1}{\gamma}} \tag{IV.01}$$

putting

$$\gamma = 1{\cdot}4.$$

Select T_{nom} = nearest temperature to $T_{s,\text{CLASSIC}}$ in Hilsenrath's tables (steps of 10 deg C).

Extract the following data from the tables:

$S^0_{1\text{ atm},Tt}$

$H^0{}_t$

$S^0_{1\text{ atm},T_{\text{nom}}}$ $\delta_{\frac{1}{2}}[S^0]\,\delta_{-\frac{1}{2}}[S^0]\,\delta_{1\frac{1}{2}}[S^0]\,\delta_{-1\frac{1}{2}}[S^0]$

$H^0{}_{\text{nom}}$ $\delta_{\frac{1}{2}}[H^0]$.

The δ's here are the tabulated first differences for changes in temperature from T_{nom}. In the present Appendix we shall make use of the second differences which are calculated as shown in Table 2 below. The extra complexity is justified by the increased precision of the S^0 data for Ideal Air which is tabulated to four decimal places (i.e. 1 in 200000) instead of three decimal places for Real Air.

TABLE 2

$x = T$	$f[x] = S^0$	First differences $\delta[S^0]$	Second differences $\delta^2[S^0]$
x_{-2}	S^0_{-2}		
		$\delta_{-1\frac{1}{2}} = S^0_{-1} - S^0_{-2}$	
x_{-1}	S^0_{-1}		δ^2_{-1} $\delta_{-\frac{1}{2}} - \delta_{-1\frac{1}{2}}$
		$\delta_{-\frac{1}{2}} = S^0_0 - S^0_{-1}$	
$T_{\text{nom}} = x_0$	S^0_0		$\delta^2_0 = \delta_{\frac{1}{2}} - \delta_{-\frac{1}{2}}$
		$\delta_{\frac{1}{2}} = S^0_1 - S^0_0$	
x_1	S^0_1		$\delta^2_1 = \delta_{1\frac{1}{2}} - \delta_{\frac{1}{2}}$
		$\delta_{1\frac{1}{2}} = S^0_2 - S^0_1$	
x_2	S^0_2		

(N.B. The index $^{(0)}$ denotes Ideal Air.)

The tabular interval used throughout Hilsenrath's tables is:

$$h = x_2 - x_1 = x_1 - x_0, \text{ etc.}$$

$$= 10 \text{ deg C.} \tag{IV.02}$$

For enthalpy, it was sufficient to read only a single first difference $\delta_{\frac{1}{2}}\,[H^0]$, since these differences varied very little with temperature (and are independent of pressure).

Path A → B → C → D.

The general equation for Ideal Air entropy change is found from Equation (II.08) of Appendix II by putting $Z = 1$ and $\dfrac{\partial Z}{\partial T} = 0$:

$$\frac{dS^0}{R} = \frac{Cp^0}{R}\frac{dT}{T} - \frac{dP}{P}. \tag{IV.03}$$

Hence for the path A → B at constant temperature T_t (committing the gas constant R to memory):

$$S_t{}^0 - S^0_{1\text{ atm},Tt} = -ln\frac{P_t}{1} \tag{IV.04}$$

or,

$$(S_{1\text{ atm},Tt} - S_t{}^0) = ln\frac{P_t}{1} \tag{IV.05}$$

For the path B→C, the entropy change is given by the tabulated data:

$$(S^0_{1\text{ atm},T_{\text{nom}}} - S^0_{1\text{ atm},Tt}) \tag{IV.06}$$

And for the path C→D we have again from Equation (IV.03):

$$(S^0_{\text{nom}} - S^0_{1\text{ atm},T_{\text{nom}}}) = -ln\frac{P_s}{1}. \tag{IV.07}$$

Hence for the complete path A→B→C→D, adding up the separate legs from Equations (IV.05), (IV.06), (IV.07) we have:

$$(S^0_{\text{nom}} - S_t{}^0) = ln\,P_t + (S^0_{1\text{ atm},T_{\text{nom}}} - S^0_{1\text{ atm},Tt}) - ln\,P_s \tag{IV.08}$$

$$S^0_{\text{nom}} = S_t{}^0 - (S^0_{1\text{ atm},Tt} - S^0_{1\text{ atm},T_{\text{nom}}}) + ln\left(\frac{P_t}{P_s}\right) \tag{IV.09}$$

Path D → E *in Figure* 4.

We need to find the temperature $T_{s,\text{IDEAL}}$ at constant pressure P_s, at which the entropy S^0_s is equal to the initial entropy $S_t{}^0$ (i.e. an isentropic process). This is achieved by a reverse interpolation of second degree, since the precision of the S^0 data (1 part in 200 000) justifies the better-than-linear technique. Thus in standard notation for numerical methods:

$$f_p = f_0 + p\,\delta_{\frac{1}{2}} + \frac{1}{4}(p^2 - p)(\delta_0^2 + \delta_1^2). \tag{IV.10}$$

In our present Notation, Equation (IV.10) becomes:

$$S_s^0 = S_{\text{nom}}^0 + p\,\delta_{\frac{1}{2}}[S^0] + \frac{1}{4}(p^2 - p)\left(\delta_0^2[S^0] + \delta_1^2[S^0]\right) \tag{IV.11}$$

where

$$p = \frac{T_s - T_{\text{nom}}}{10} \text{ exactly} \tag{IV.12}$$

Equations (IV.11), (IV.12) are solved for T_s by iteration, using successive approximations for p.

If it should happen that $T_s < T_{\text{nom}}$, then new values are defined thus:

$$T'_{\text{nom}} = T_{\text{nom}} - 10\,\text{deg} \tag{IV.13}$$

$$S^{0\prime}_{\text{nom}} = S^0_{\text{nom}} - \delta_{-\frac{1}{2}}[S^0] \tag{IV.14}$$

$$H^{0\prime}_{\text{nom}} = H^0_{\text{nom}} - \delta_{\frac{1}{2}}[H^0] \tag{IV.15}$$

($\delta_{\frac{1}{2}}[H^0]$ is a sufficiently close approximation to the $\delta_{-\frac{1}{2}}[H^0]$). Thus each of the differences required by Equation (IV.11) is taken from the next level in Table 2. The corresponding computational path would be C′ → D′ → E′ in Figure 4 for this case.

Having obtained the temperature $T_{s,\,\text{IDEAL}}$ by Equations (IV.11), (IV.12) we proceed to calculate enthalpy by linear interpolation which is sufficiently precise. Thus:

$$H_s^0 = H_{\text{nom}}^0 + \frac{\delta_{\frac{1}{2}}[H^0]}{10}(T_s - T_{\text{nom}}) \tag{IV.16}$$

or

$$H_s^0 = H_{\text{nom}}^{0\prime} + \frac{\delta_{\frac{1}{2}}[H^0]}{10}(T_s - T'_{\text{nom}}) \tag{IV.17}$$

Finally, the Ideal Air isentropic velocity is obtained from an equation similar to Equation (III.23) developed in Appendix III:

$$V_{\text{IDEAL}} = \sqrt{156816\,(H_t^0 - H_s^0)}\ m/s \tag{IV.18}$$

where both H_t and H_s are non-dimensional values as discussed in Appendix III.

Hence from Equation (IV.18) above and Equations (III.24), (III.25) at Appendix III, we obtain the isentropic velocity ratio, $V_{\text{IDEAL}}/V_{\text{CLASSIC}}$.

Since the compressibility is:

$$Z = \frac{P_s}{\rho R\,T_s} = 1 \tag{IV.19}$$

for both Ideal Air and Classic Air, we obtain the ratio of mass flow intensities as:

$$\frac{(\rho V)_{\text{IDEAL}}}{(\rho V)_{\text{CLASSIC}}} = \left(\frac{T_{s,\text{CLASSIC}}}{T_{s,\,\text{IDEAL}}}\right)\left(\frac{V_{\text{IDEAL}}}{V_{\text{CLASSIC}}}\right) \tag{IV.20}$$

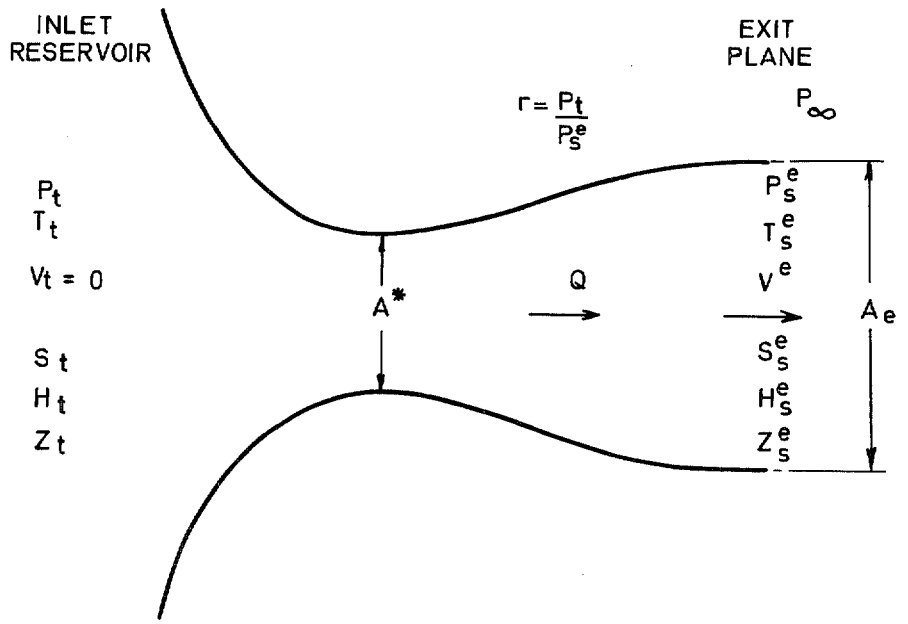

ISENTROPIC EXPANSION PROCESS

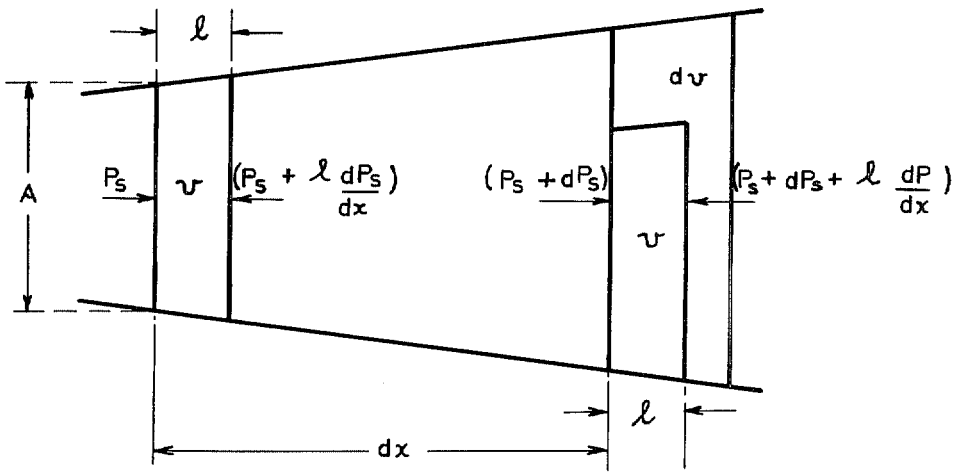

FLOW WITHIN A SECTION OF NOZZLE

FIG. 1. Basic principles. Propelling-nozzle performance (*see* Appendix 1).

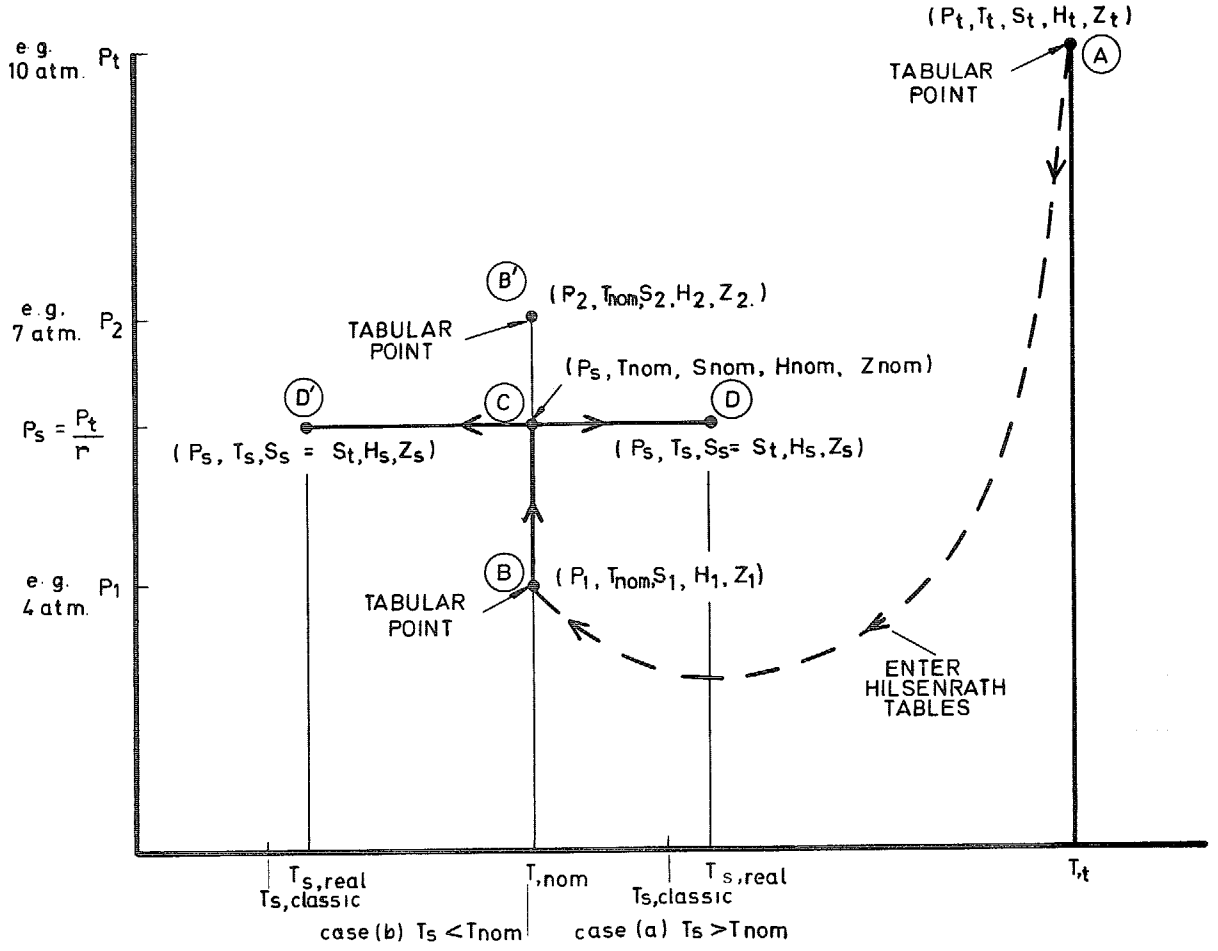

FIG. 2. Computation path. Real-air calculations (*see* Appendices II and III).

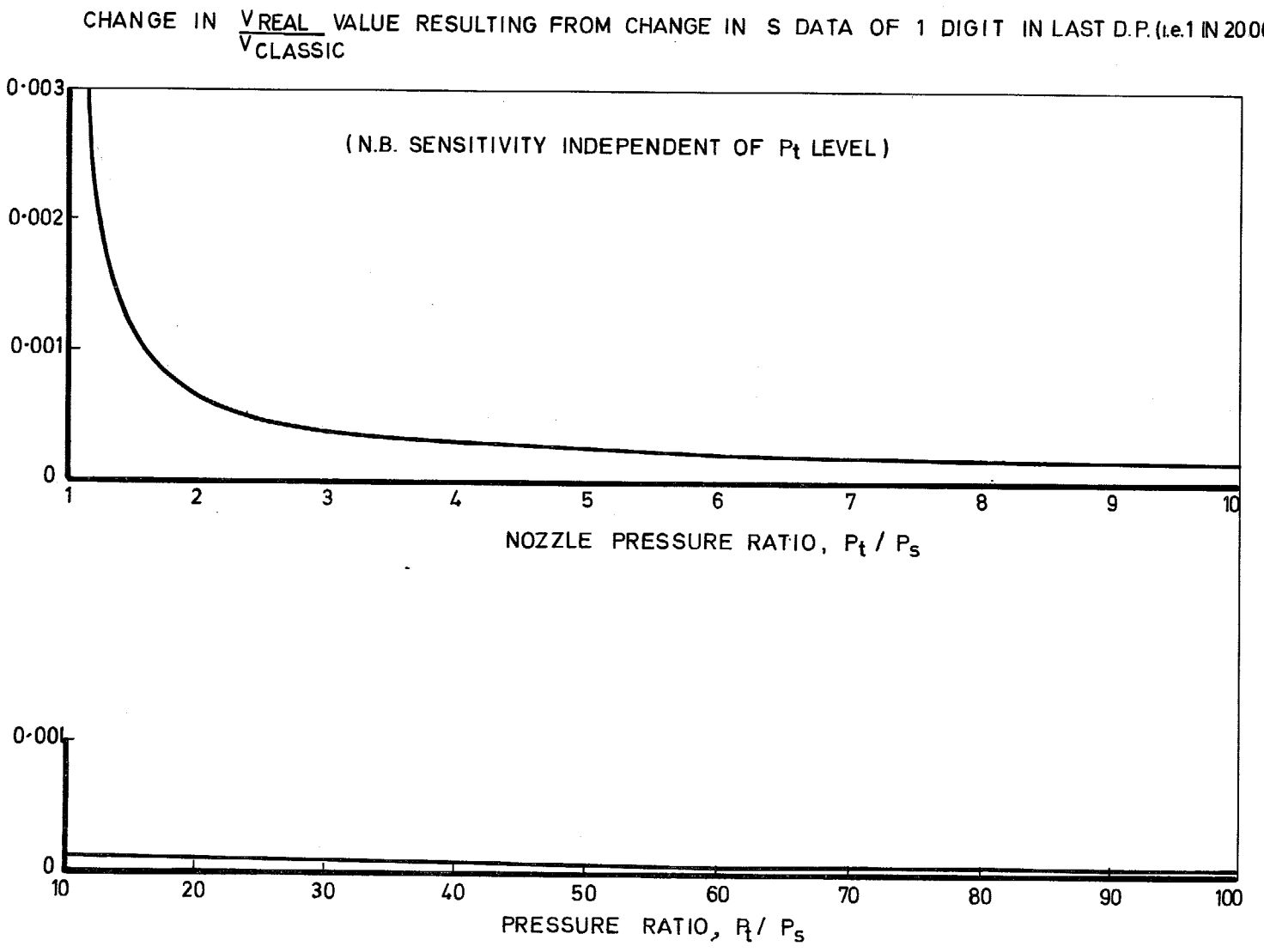

FIG. 3. Sensitivity of V_{REAL} calculation. 1 digit error in S-data.

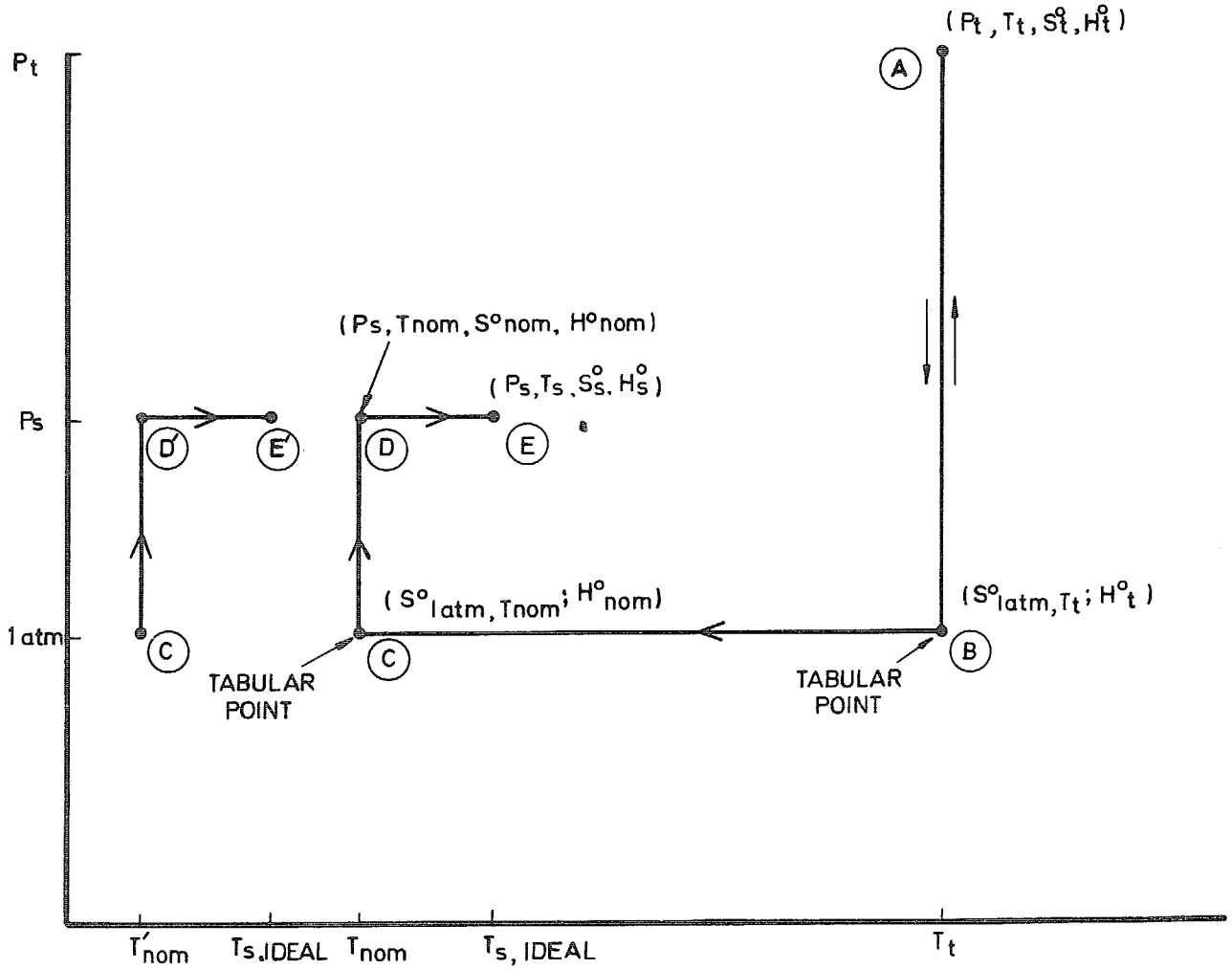

FIG. 4. Computation path. Ideal-air calculations (*see* Appendix IV).

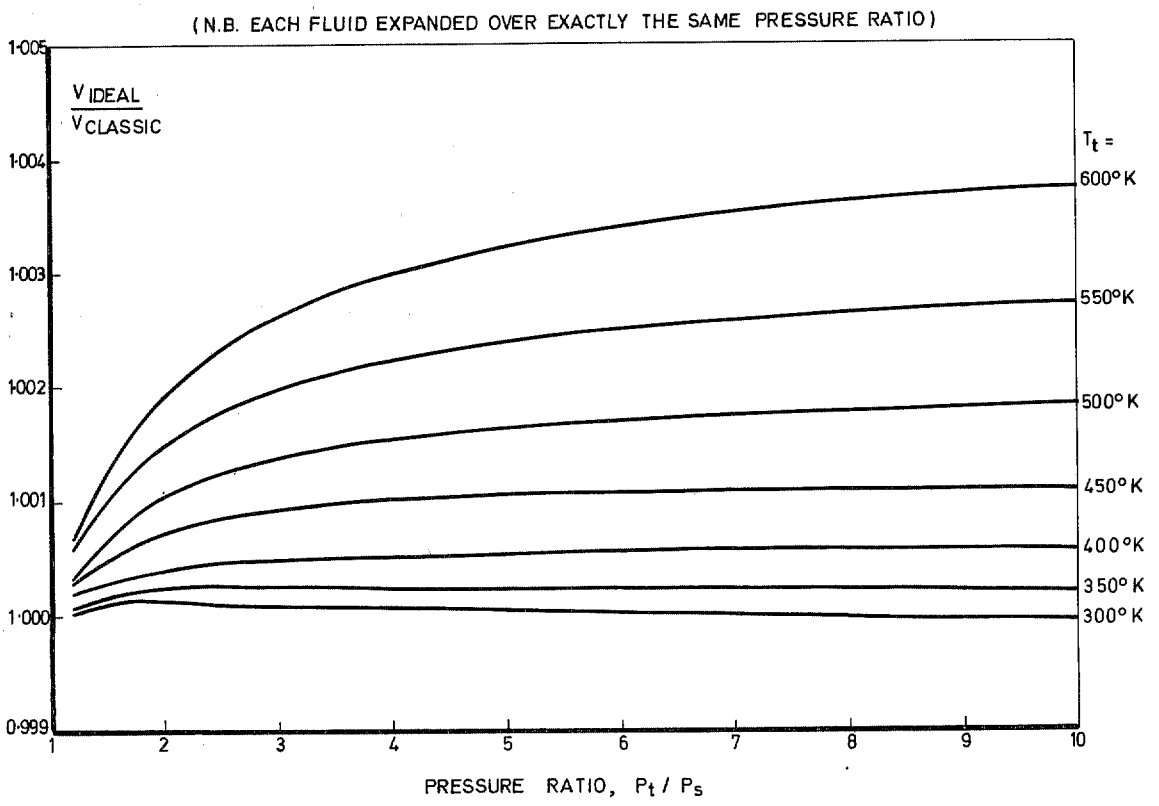

FIG. 5. Ideal air: classic air. Isentropic velocity ratio (at $P_t = 10$ atm).

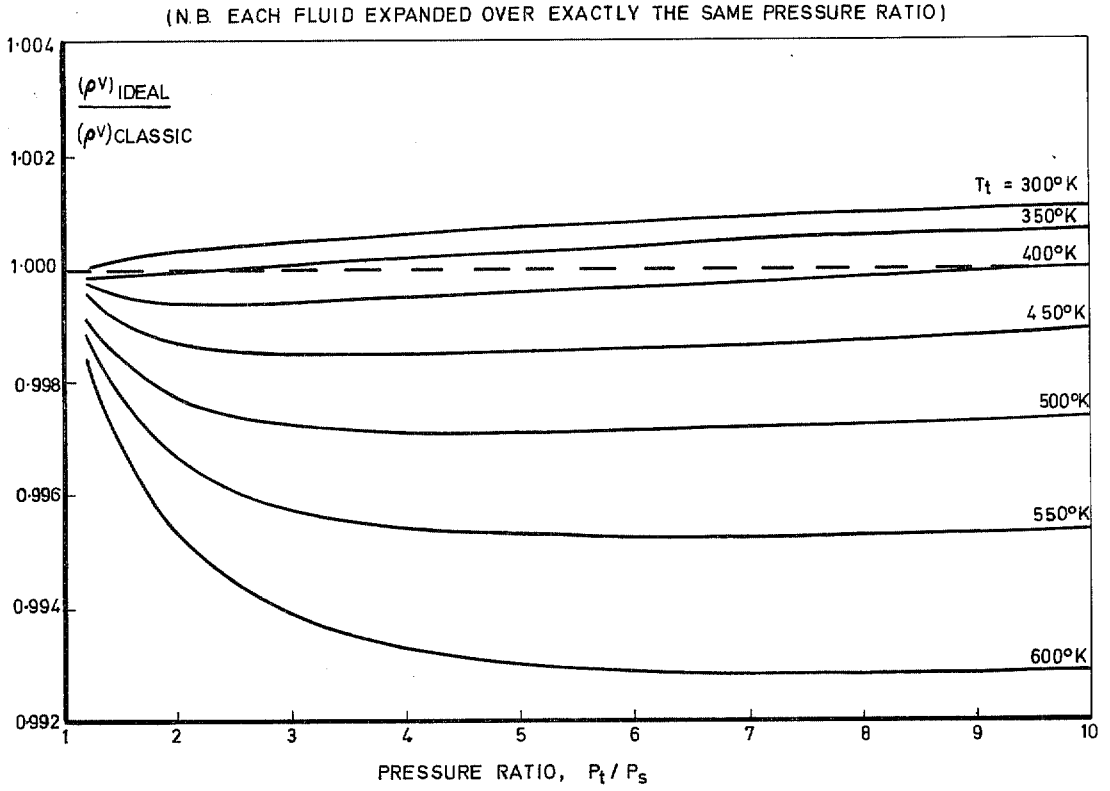

FIG. 6. Ideal Air: classic air. Isentropic mass-flow ratio (at $P_t = 10$ atm).

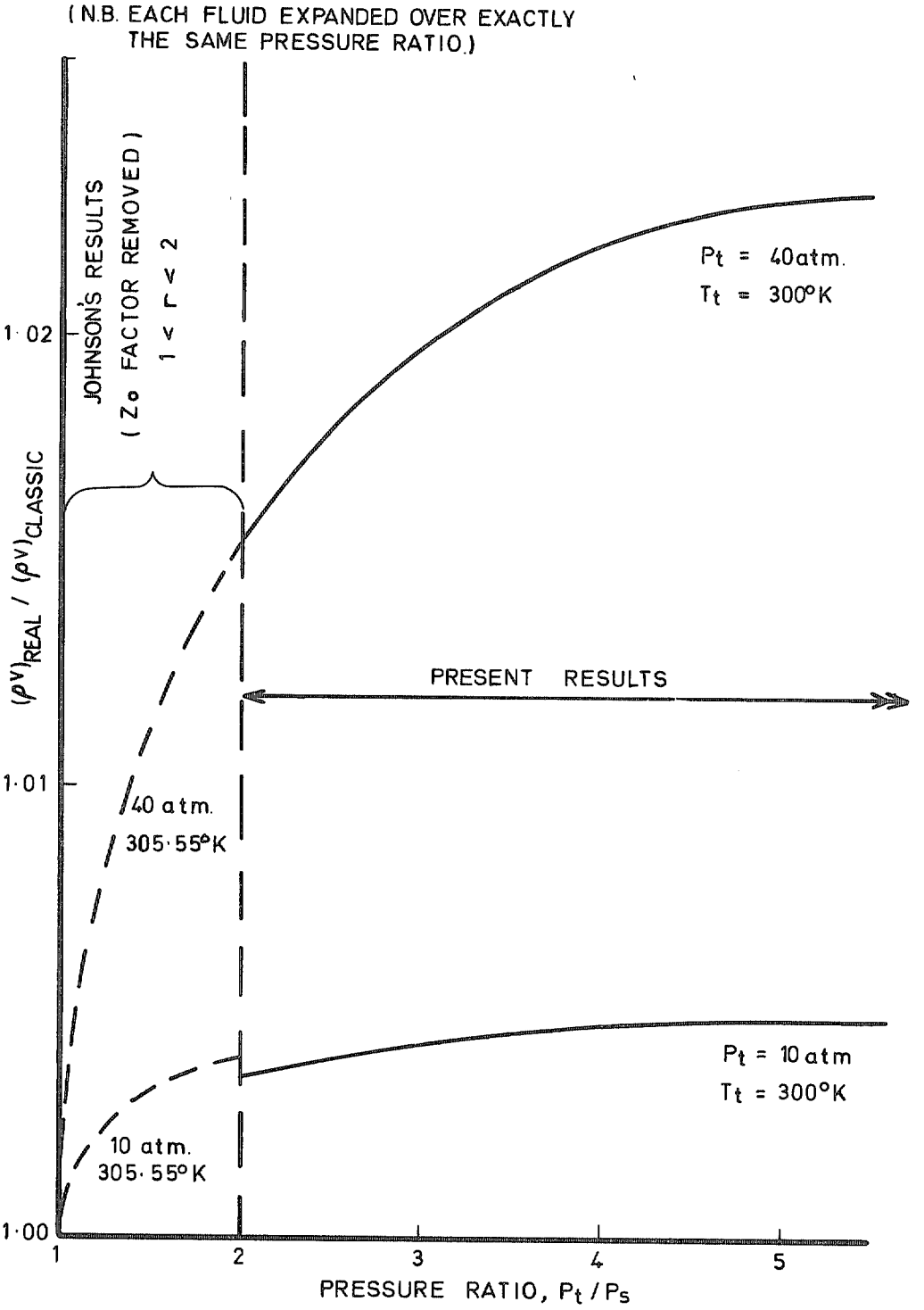

FIG. 7. Real air: classic air isentropic mass-flow ratio. Comparison of calculation methods.

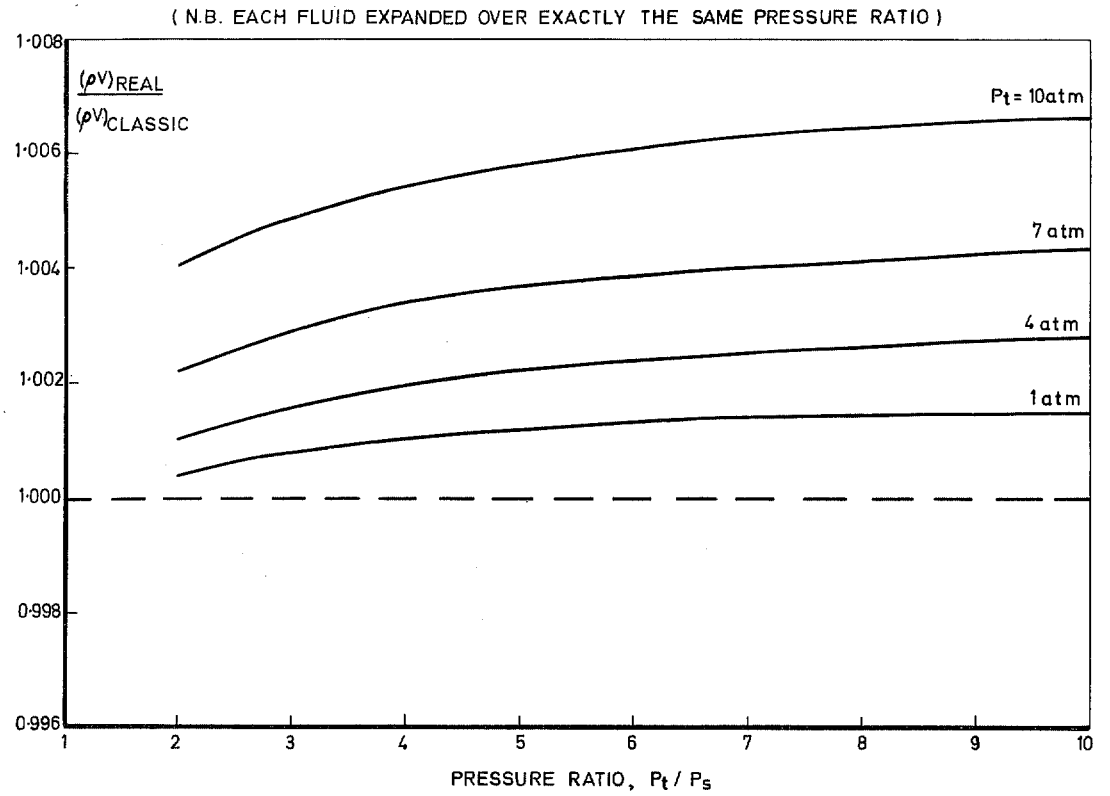

FIG. 8. Real air classic air isentropic mass-flow ratio. Effect of inlet pressure (at $T_t = 290$ deg K).

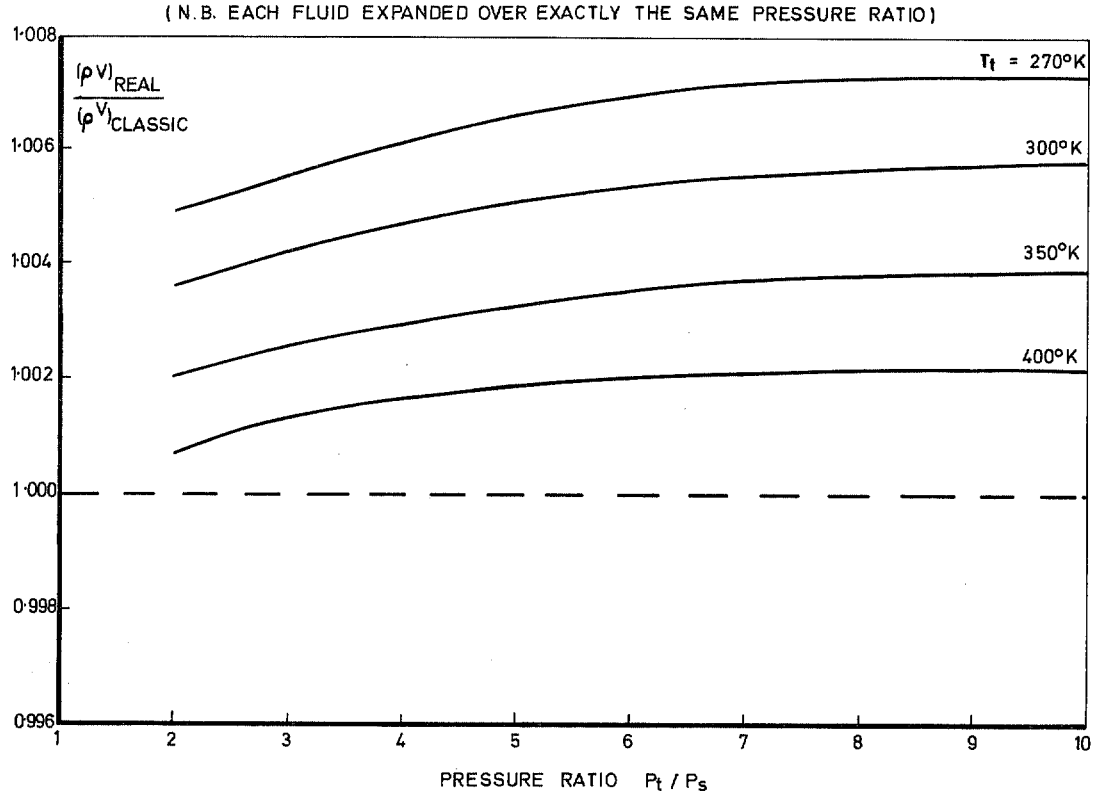

FIG. 9. Real air: classic-air isentropic mass-flow ratio. Effect of inlet temperature (at $P_t = 10$ atm).

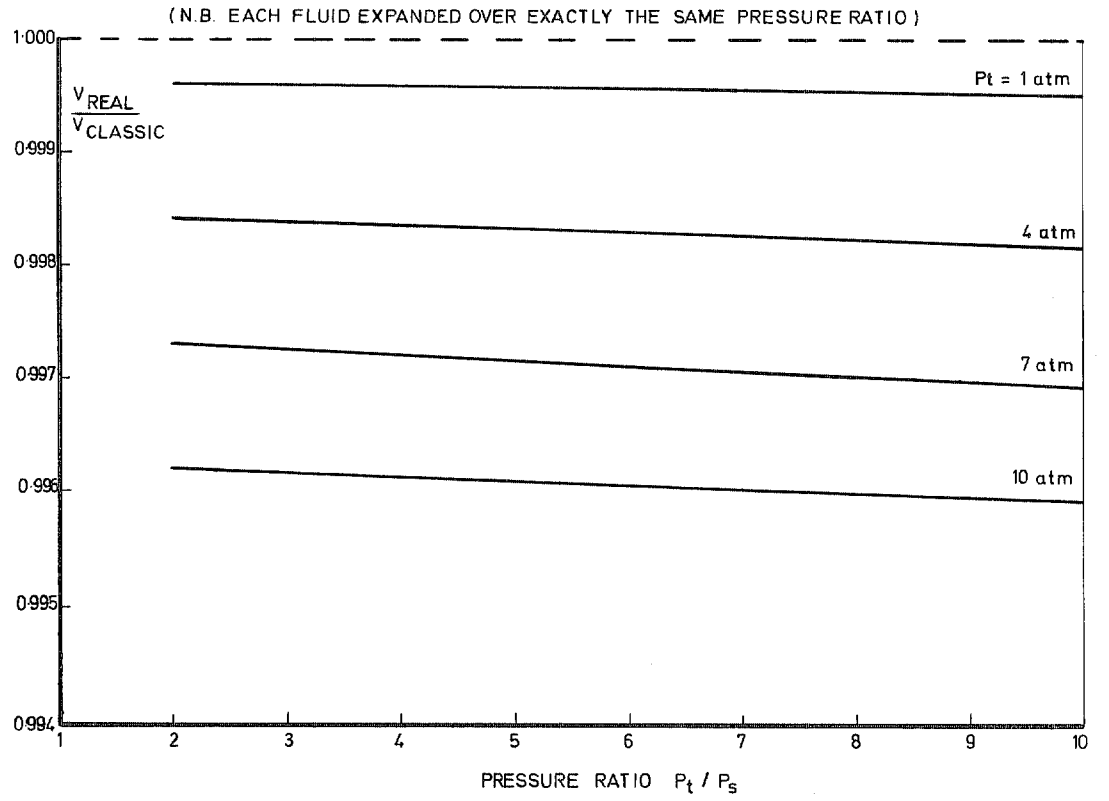

FIG. 10. Real air: classic-air isentropic velocity ratio. Effect of inlet pressure (at $T_t = 290$ deg K).

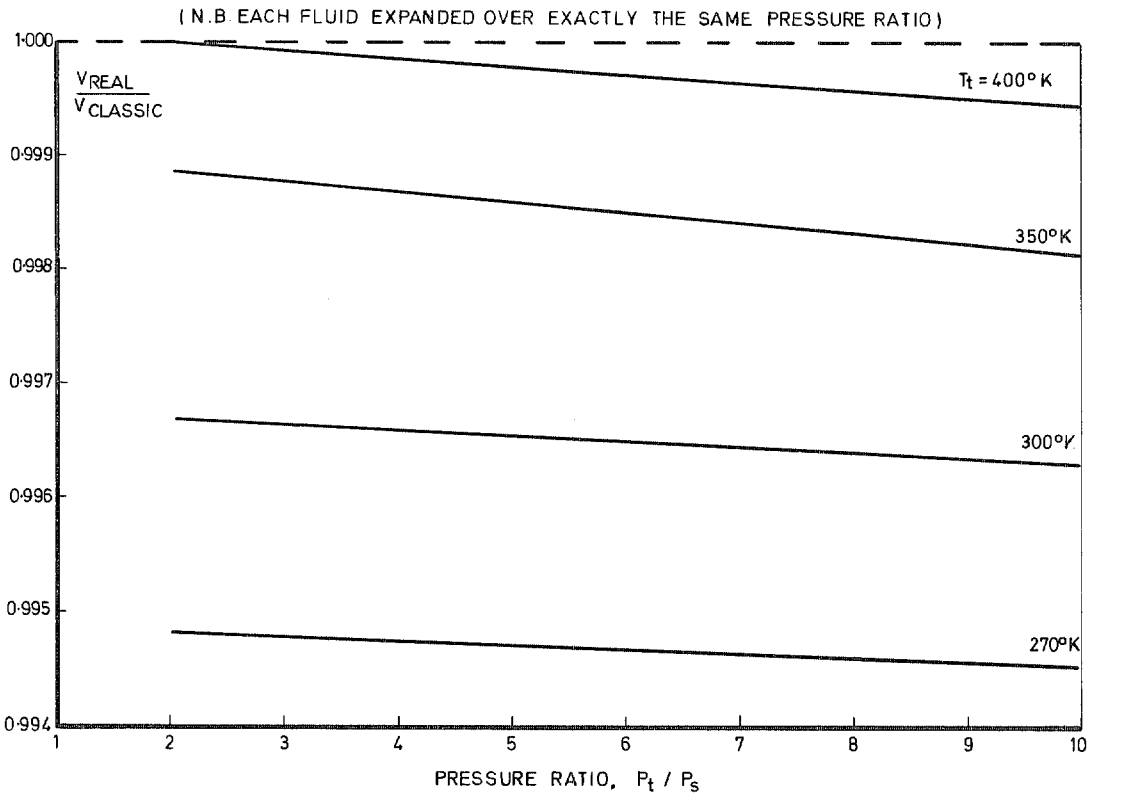

FIG. 11. Real air: classic air isentropic velocity ratio. Effect of inlet temperature (at $P_t = 10$ atm).

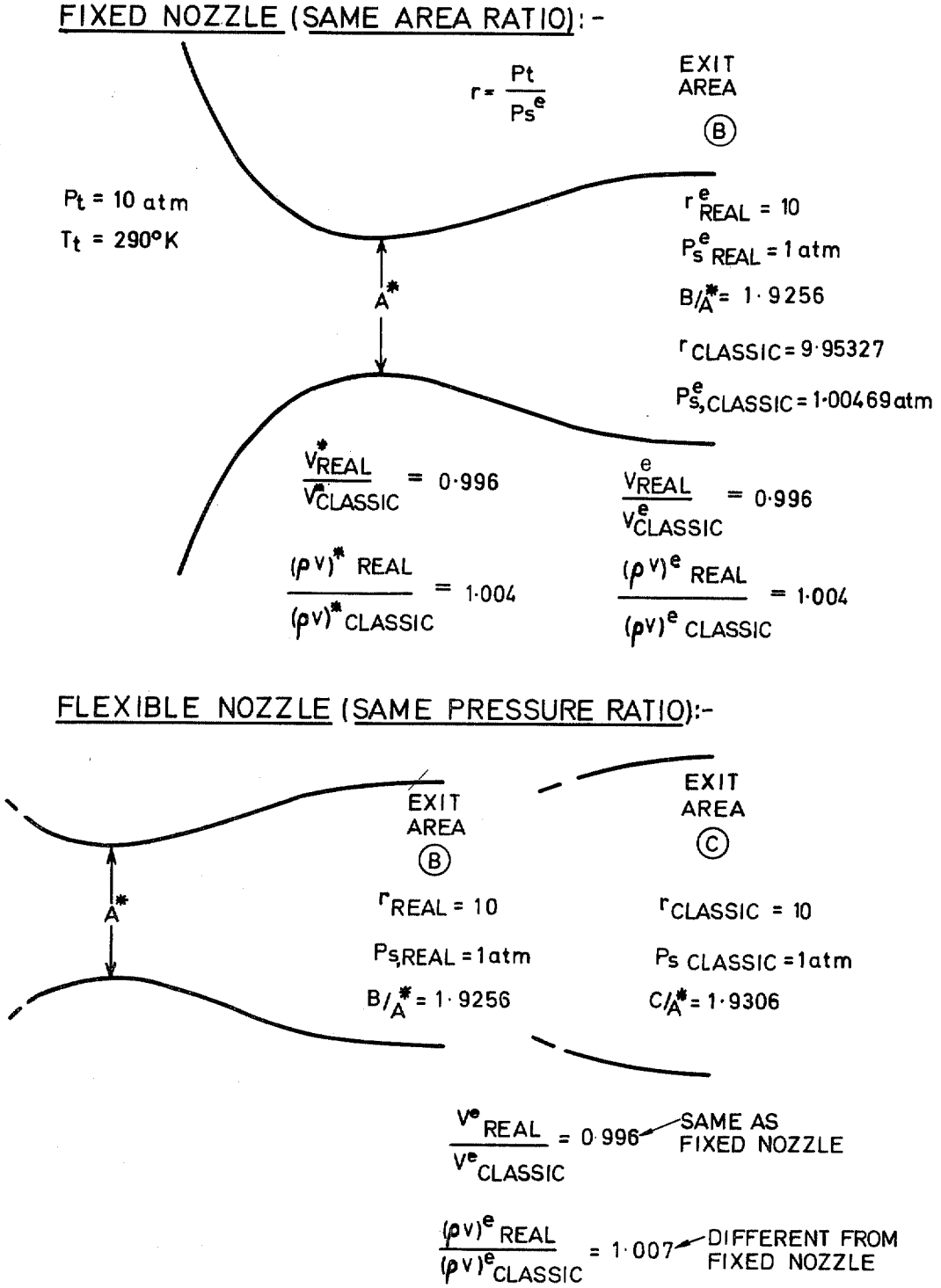

FIG. 12. Comparison of fixed and flexible nozzles.

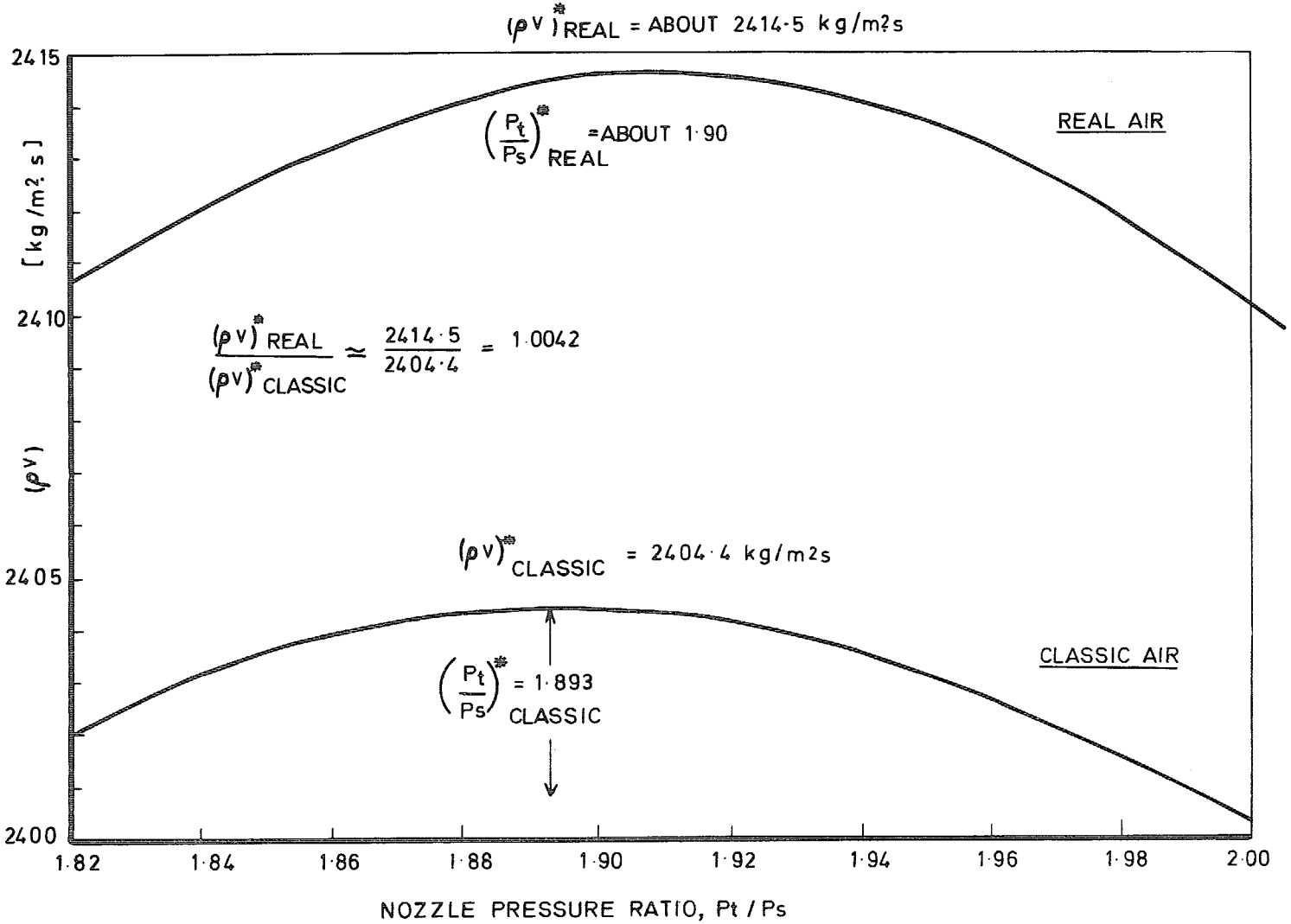

FIG. 13. Isentropic mass-flow intensities. Near choking conditions (at $P_t = 10$ atm, $T_t = 290$ deg K).

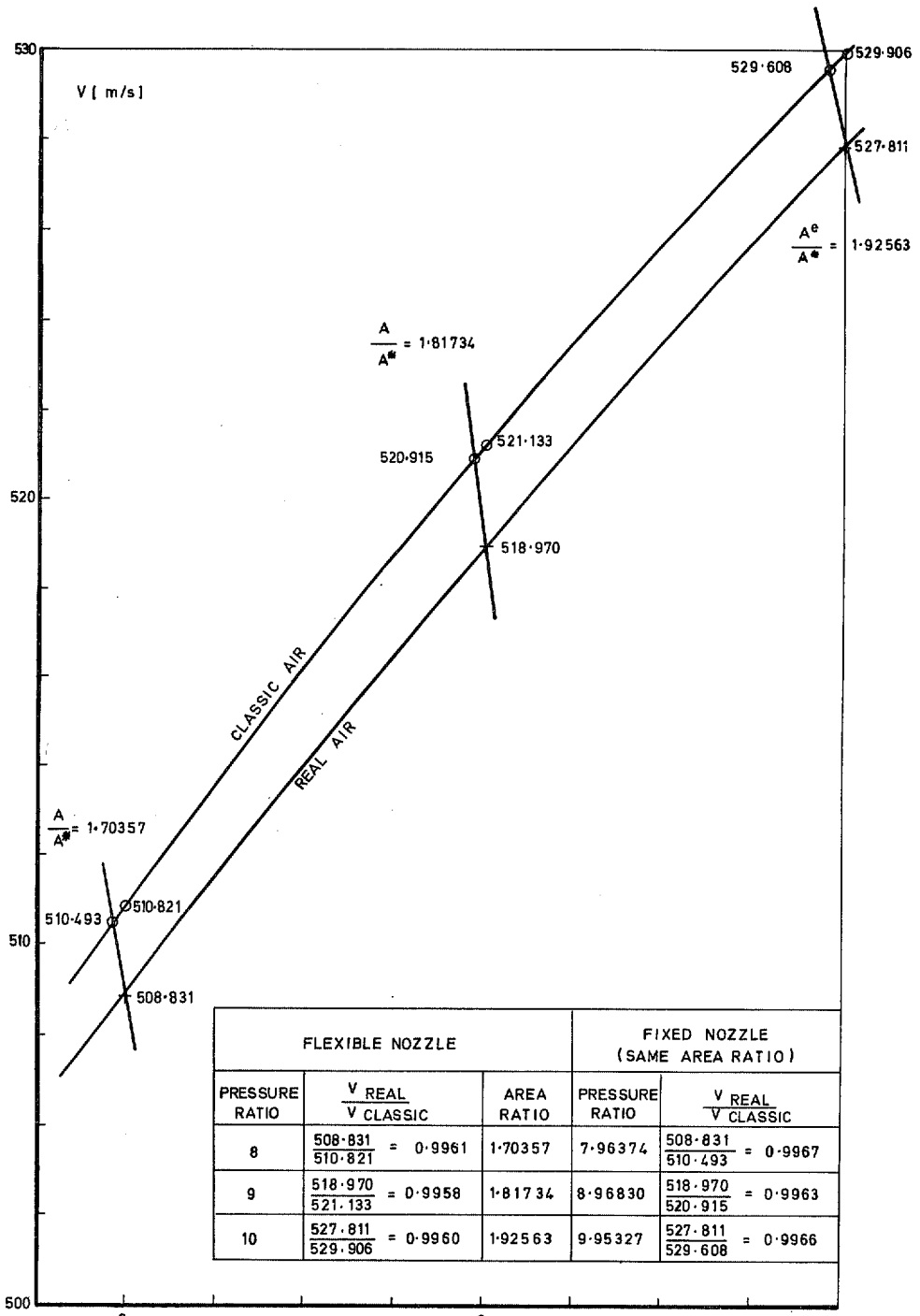

FLEXIBLE NOZZLE			FIXED NOZZLE (SAME AREA RATIO)	
PRESSURE RATIO	$\frac{V \text{ REAL}}{V \text{ CLASSIC}}$	AREA RATIO	PRESSURE RATIO	$\frac{V \text{ REAL}}{V \text{ CLASSIC}}$
8	$\frac{508·831}{510·821}$ = 0·9961	1·70357	7·96374	$\frac{508·831}{510·493}$ = 0·9967
9	$\frac{518·970}{521·133}$ = 0·9958	1·81734	8·96830	$\frac{518·970}{520·915}$ = 0·9963
10	$\frac{527·811}{529·906}$ = 0·9960	1·92563	9·95327	$\frac{527·811}{529·608}$ = 0·9966

FIG. 14. Real air and classic air isentropic velocities at exit from fixed con-di nozzles. (At $P_t = 10_{\text{atm}}$, $T_t = 290$ deg K).

Printed in Wales for Her Majesty's Stationery Office by Allens Printers (Wales) Limited

Dd. 129527 K 5

Published by
HER MAJESTY'S STATIONERY OFFICE

To be purchased from
49 High Holborn, London W.C.1
423 Oxford Street, London W.1
13A Castle Street, Edinburgh 2
109 St. Mary Street, Cardiff CF1 1JW
Brazennose Street, Manchester 2
50 Fairfax Street, Bristol 1
258 259 Broad Street, Birmingham 1
7 11 Linenhall Street, Belfast BT2 8AY
or through any bookseller

R. & M. No. 3522

S O. Code No. 23 3522